CHEMISTRY OF MATERIALS

Review

pubs.acs.org/cm

Routes to Nanostructured Inorganic Materials with Potential for Solar Energy Applications

Karthik Ramasamy,[‡] Mohammad Azad Malik,[†] Neerish Revaprasadu,[§] and Paul O'Brien*[,†]

[‡]Center for Materials for Information Technology, The University of Alabama, Tuscaloosa, Alabama 35487, United States

[†]The School of Chemistry and the School of Materials, The University of Manchester, Oxford Road, Manchester M13 9PL, U.K.

[§]Department of Chemistry, The University of Zululand, Private Bag X1001, Kwadlangezwa 3886, South Africa

ABSTRACT: Recent advances in nanotechnology could facilitate the production of cheaper solar cells. This review describes synthetic routes to various nanostructured materials that are potentially useful in photovoltaic applications. We have focused on materials that are based on earth abundant elements and/or those that are held to have lower toxicity. Methods to synthesize binary chalcogenides with variable stoichiometries such as iron sulfide, copper sulfide, and nickel sulfide are described in detail. Other important photovoltaic materials such as cadmium telluride and lead sulfide are also covered. Methods to prepare emerging materials such as tin sulfide and bismuth sulfide are also discussed. Finally routes to ternary materials, e.g. copper indium sulfide and/or selenide and the quaternary material copper zinc tin sulfide, are discussed.

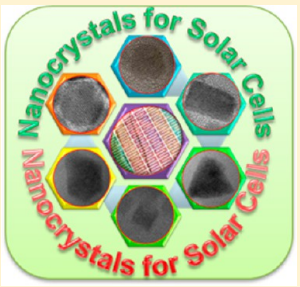

KEYWORDS: *nanostructrures, solar energy, binary, ternary and quaternary chalcogenides*

INTRODUCTION

Fossil fuels have been the main source of energy for the development of humankind and the 20th century which could be described as 'the century of man's love for oil'. Even in the 21st century, the energy mix of almost all the countries is dominated by fossil fuels. Nuclear energy has emerged as another important energy source. However the accident at Fukusima, Japan has unfortunately led some countries to abandon nuclear power.

The sun is the most abundant source of energy, and the energy striking the earth's surface in one hour is estimated to be more than the total energy consumed on the planet in a year.[1] Photovoltaic devices convert solar energy directly into usable electric power. Becquerel discovered the photovoltaic effect in 1839. However, more than 100 years later, Chapin, Pearson, and Fuller of Bell Telephone Laboratories first demonstrated a viable crystalline silicon-based solar cell in 1954.[2] This event may be regarded as the beginning of commercial photovoltaics. Since then a steady and substantial growth in this technology has been observed. However there has been a rapid growth in the photovoltaic industry during the past decade due to an increase in oil prices worldwide and the heightened awareness of the environmental impacts of conventional energy technologies. Photovoltaics have the potential to ensure a sustainable and environmentally benign energy supply system for the 21st century. It may also enhance energy security due to its global availability.

The use of nanocrystals for the large-scale fabrication of films with applications in solar energy conversion and other optoelectronic applications is an emerging area of research. Compared with physical deposition techniques, the application of suitable inorganic colloidal nanocrystal inks to produce solar cells with potentially lower fabrication cost makes the solution route more attractive. The size, shape, composition, monodispersity, and surface properties of the nanocrystals are important in exploiting their novel properties for solar cell applications. A great emphasis is placed on the synthetic methods that produce uniform nanocrystals, including hydrothermal/solvothermal approaches, the single-source precursor approach, the hot-injection approach, and the template-directed method.[3,4] Overviews of recent research into the synthesis, properties, and application of nanocrystals have been reported.[5−8]

This review will cover recent advances in the synthetic approaches to semiconductor nanomaterials, particularly those based on earth abundant and low toxicity elements for photovoltaic applications.

BINARY CHALCOGENIDES

Iron Sulfide. Iron sulfide exists in various and variable stoichiometries including FeS_2, Fe_2S_3, Fe_3S_4, Fe_7S_8, $Fe_{1-x}S$, FeS, and $Fe_{1+x}S$. All these sulfides have either the NiAs-$Cd(OH)_2$ or pyrite structures.[9] Among them FeS_2 occurs in two forms namely the pyrite and marcasite. Pyrite FeS_2 is a nonmagnetic semiconductor with an optical band gap of 0.9 eV.[10] It is of interest as a cheap and less toxic material for solar cells. There has been considerable interest in the synthesis of nanocrystals of different compositions of iron sulfides shown in recent years. Fe_7S_8 nanowires were synthesized by Rao et al. in a solvothermal experiment using $FeCl_2{\cdot}4H_2O$, thioacetamide and ethylenediamine in Teflon-lined stainless steel autoclave for 4 days at 180 °C.[11] Isolated nanowires were 40−180 nm in

Received: April 25, 2013
Revised: May 30, 2013
Published: June 18, 2013

   dx.doi.org/10.1021/cm401366q | *Chem. Mater.* 2013, 25, 3551−3569

diameter with several micrometers length. A hydrothermal experiment with ammonium iron sulfate hexahydrate and cysteine produced greigite (Fe_3S_4) microrods.[12] Similar experiments with thiohydracrylic acid or thioacetamide gave marcasite FeS_2 or mixtures of FeS_2, Fe_3S_4, or Fe_9S_{11}. Figure 1 shows SEM images of marcasite FeS_2 prepared using thiohydracrylic acid or thioacetamide as the sulfur source.

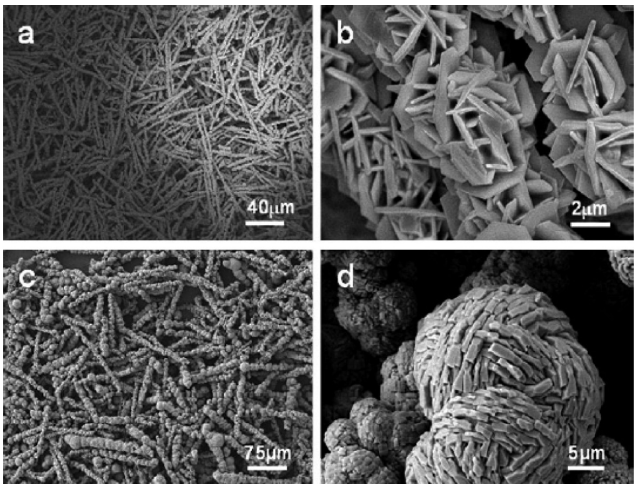

Figure 1. SEM images of marcasite FeS_2 microrods prepared using different sulfur precursors at 180 °C in the presence of a magnetic field. a,b) Low- and high-magnification images of microrods constructed by hexagonal nanoplates synthesized using thiohydracrylic acid as the sulfur precursor. c,d) Low- and high-magnification images of microrods composed of squarelike bricks prepared using thioacetamide as the sulfur precursor [Reprinted from ref 12 with permission from John Wiley and Sons].

Vanitha and O'Brien synthesized pyrrhotite type Fe_7S_8 and greigite type Fe_3S_4 nanoparticles from $[N^nBu_4]_2[Fe_4S_4(SPh)_4]$ as single source precursor by varying solvent.[13] Interestingly, the precursors yielded pyrrhotite Fe_7S_8 nanocrystals in octylamine at 180 °C but greigite Fe_3S_4 nanocrystals in dodecylamine at 200 °C. Both nanocrystals are spherical in shape with sizes of 5.6 nm (pyrrhotite) and 2.5 to 4.5 nm (greigite) and both are superparamagnets. Following this work, Han and Gao used diethyldithiocarbamate complexes $[Fe(ddtc)_2(Phen)]$ and $[Fe(ddtc)_3]$ for the synthesis of iron sulfide nanocrystals.[14] Thermolysis of $[Fe(ddtc)_2(Phen)]$ in oleylamine at 280 °C gave Fe_7S_8 hexagonal nanosheets (500–800 nm), whereas $[Fe(ddtc)_3]$ yielded Fe_3S_4 nanosheets (100–500 nm) under the same experimental conditions. Min et al. reported a solvothermal reaction for the synthesis of nano $Fe_{0.98}S$.[15] Ferric chloride, L-cysteine, water, and ethylenediamine were kept at 200 °C for 24 h. The morphology of the material could be changed from nanofibers to nanoflowers by varying the experimental conditions. Wadia et al. prepared pure pyrite FeS_2 nanocrystals using $[Fe((S)_2P(C_2H_5O)_2)_3]$ as single source precursors.[16] In this method, the precursor was decomposed with hexadecyltrimethylammonium bromide (CTAB) in a Teflon lined-stainless steel acid digestion bomb at 200 °C. The bandgap of synthesized pyrite nanocrystals was reported as 0.95 ± 0.1 eV based on X-ray absorption and emission spectroscopy measurements.

Lin et al. constructed a hybrid solar cell using poly(3-hexylthiophene) (P3HT) and iron sulfide (FeS_2) nanocrystals.[17] FeS_2 nanocrystals were synthesized by reacting $FeCl_2$, 1,2-hexadecanediol, and oleylamine at 100 °C for 1 h and followed by injection of sulfur in oleylamine. The mixture was kept at 220 °C for 1 h. The synthesized nanoparticles were ~10 nm in diameter. A hybrid solar cell was fabricated by spin coating P3HT/FeS_2 onto ITO. The cell showed a short circuit current density (Jsc) of 0.85 mA cm^{-2}, an open circuit voltage of 0.44 V, and a fill factor (FF) of 0.42 with power conversion efficiency (η) of 0.16%.

Recently, Puthussery et al. reported a hot injection method for the synthesis of pyrite nanoparticles.[18] In their method sulfur was dissolved in diphenyl ether and injected into a vessel containing $FeCl_2$ and octadecylamine preheated at 220 °C. The as-synthesized nanoparticles were oblate and spherical in shape with sizes of 5–20 nm. Figure 2 shows transmission and high resolution transmission electron microscope images of FeS_2 nanoparticles. Arrows in Figure 2 indicate doughnutlike morphology with holes or depressions. These nanoparticles were used as nanoinks for the preparation of thin films by the dip-coating process. Fe_3S_4 and $Fe_{1-x}S$ nanostructures can also be produced by the thermal decomposition of iron polysulfide $[Fe(N\text{-MeIm})_6]S_8$ in oleylamine.[19] Pyrite (FeS_2) nanodendrites or nanocubes were produced by injection of sulfur in oleylamine into a vessel containing $FeCl_2$-oleylamine at 100 °C followed by heating to 220 °C.[20] Recently, Bi et al. reported pyrite nanocrystals synthesized using tri-n-octylphosphine oxide (TOPO) have better air stability than FeS_2 nanocrystals synthesized without TOPO.[21] TOPO capped nanocrystals were synthesized by the hot injection method. Sulfur in oleylamine was injected into iron precursor solution prepared by mixing TOPO and oleylamine with $FeCl_2$. Isolated nanocrystals were shown to be uniform 60 nm cubes. The size of the nanocrystals can be varied between 60 and 200 nm by varying the quantity

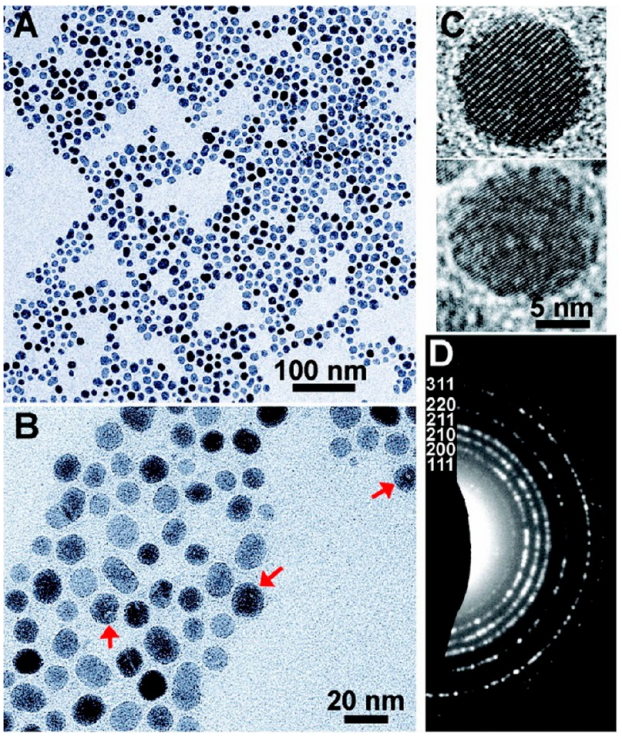

Figure 2. TEM, HRTEM, and ED images of FeS_2 nanocrystals. [Reprinted from ref 18with permission from American Chemical Society].

dx.doi.org/10.1021/cm401366q | Chem. Mater. 2013, 25, 3551–3569

of TOPO. A similar hot injection method was adopted for the synthesis of Fe_3S_4 nanocrystals.[22] The acetylacetonate complex of iron [$Fe(acac)_2$] was heated to 300 °C in hexadecylamine, to which solution of elemental sulfur dissolved in oleylamine was injected. Spherical nanoparticles with an average diameter of 6.5 ± 0.5 nm were obtained.

The O'Brien group carried out a comparative study of the thermolysis reaction for the synthesis of iron sulfide nanoparticles from symmetrical and unsymmetrical dithiocarbamate complexes of iron(III).[23] Complexes [$Fe(S_2CNEt^iPr)_3$] (**1**), [$Fe(S_2CN(Hex)_2)_3$] (**2**), [$Fe(S_2CNEtMe)_3$] (**3**), and [$Fe(S_2CN(Et)_2)_3$] (**4**) were decomposed in oleylamine at 170, 230, and 300 °C. Complexes (**1**)−(**3**) yielded predominantly gregite (Fe_3S_4) and a small amount of pyrrhotite, whereas complex (**4**) gave pure gregite (Fe_3S_4). Manna et al. reported another method for the synthesis of Fe_3S_4 as nanoplates (10−20 nm lateral size).[24] The process involved heating $FeCl_2$, anhydrous $Na_2S_2O_3$, elemental sulfur, 3-methyl catechol, and octadecylamine in octadecene to 200 °C for 2 h. FeS_2 can also be synthesized with nanoplate morphology by injecting $Fe(CO)_5$ into hot oleylamine containing sulfur at different temperatures.[25] Recently, O'Brien et al. have shown that the use of iron(III) complex of 1,1,5,5-tetraisopropyl-2-thiobiuret as single source precursor for Fe_7S_8 nanostructures with different morphologies (dots, rods, or plates).[26] In the development of synthetic methods for iron sulfide nanostructures, Jin et al. reported a new method for synthesis of FeS_2 nanowires.[27] The method involved heating of steel foil under a sulfur atmosphere at 350 °C for 2 h. The FeS_2 nanowires are 4−10 nm in diameter with more than 2 μm length. Besides the growth of pyrite nanowires, a scale layer of pyrrhotite was deposited with a thickness between 440 nm and 2.3 μm.

Macpherson and Stoldt reported the synthesis of pyrite iron sulfide nanocubes by reacting $FeCl_2$ and elemental sulfur in alkylamines.[28] $FeCl_2$, and sulfur were heated to 250 °C in hexadecylamine under argon atmosphere for 3 h for the formation of nuclei. Once the nucleation of reaction was completed, the reaction vessel was cooled to room temperature to freeze the reaction. A portion of $FeCl_2$, sulfur, and oleylamine was added to the reaction vessel and reheated to 200 °C for 9 h. This process was repeated for the complete growth of pyrite nanocrystals. Nanocrystals were isolated by centrifugation and washed with chloroform. The nanocrytsals obtained by this method were of random oblate shape. However, the size distribution of the nanocrystals was improved after the second stage growth. The final FeS_2 nanocubes isolated by this method had size of 37 ± 11 nm. Absorption measurements of the nanocubes showed an indirect band gap around 1.1 eV along with two excitonic transitions at 1.9 and 3.0 eV.

Nickel Sulfide. Nickel sulfides have another system with a complex phase diagram that includes NiS, Ni_3S_4, Ni_3S_2, Ni_7S_6, Ni_9S_8, Ni_6S_5, and NiS_2.[29] Among them only NiS_2 and NiS are semiconductors. These nickel sulfides (NiS, NiS_2) find applications as a cathode material for lithium−ion batteries, a counter electrode for dye sensitized solar cells, an absorber material in thin film solar cells, and as a hydrogenation catalyst.[30−32] Nickel sulfides could be a potential competitor material for silicon in thin film solar cells.[33] Various methods have been demonstrated for the synthesis of nickel sulfide nanostructures. A hydrothermal experiment using $NiCl_2·6H_2O$ and sulfur or thiourea in ethylenediamine and hydrazine hydrate in an autoclave at 170 °C produced NiS nanorods.[34] The nanorods were 50 nm in diameter with a length of 1.7 μm. Tilley and Jefferson reported that nickel nanoparticles can be converted to nickel sulfide nanoparticles by sulfurization using H_2S/H_2.[35] Nickel sulfides of different stoichiometries can also be selectively synthesized by varying the experimental conditions such as H_2S concentration, reaction temperature, and reaction time. Nanoparticles obtained were β-Ni_3S_2, Ni_9S_8, Ni_7S_6, and β-NiS with sizes ranging from 2 to 100 nm. A solvothermal method using $Ni(OAc)_2·6H_2O$ and dithizone in ethylenediamine was shown to be a promising method for the synthesis of an urchinlike nanostructure of NiS.[36]

Yet another method was reported for the synthesis of NiS as nanorods or nanoprisms.[37,38] The method involved the thermolysis of nickel thiolate precursor in octonate. The nanorods obtained were 33.9 ± 8.6 nm in length and 8.1 ± 1.6 nm in width, but the nanoprisms were polydispersed. Shells of Ni_3S_2 (5−10 nm) were grown on a Ni core (10−15 nm) by sulfurization using thiourea.[39] The nickel nanotemplate was synthesized by the reduction of $NiCl_2·6H_2O$ using hydrazine in polyvinyl pyrrolidone (PVP); Ni_3S_2 shells were grown on to that core by reaction with thiourea at 168 °C. Another templated growth was reported for NiS nanoparticles by Morris et al.[40] NiS nanoparticles were grown on anodic alumina templates by decomposing nickel xanthate complex in supercritical CO_2 at 450 °C. Nanowires obtained after dissolution of alumina template were composed of around 20−25 nm-sized nanoparticles. Magnetic measurements on these nanoparticles showed superparamagnetic behavior (T_b = 170 K) at room temperature with T_c around 390 K. Hollow spheres of NiS were synthesized using silica nanosphere as templates.[41] Figure 3 shows SEM and TEM images of core−shell structured SiO_2@nickel silicate nanospheres. The nanospheres were 400 nm in diameter with about 10 nm thickness. Another method for the synthesis of hollow NiS spheres was reported.[42] Na_2SO_4 or Na_2S was used to sulfurize $Ni(OH)_2$ in a Teflon-lined autoclave at 180 °C for the synthesis of NiS hollow spheres. Tatsumisago et al. reported a thermal decomposition method for different stoichiometries of nickel sulfide nanostructures.[43] The synthetic method involves thermal decomposition of nickel acetylacetonate in 1-dodecanethiol in a high boiling solvent (oleylamine, trioctylamine, oleic acid, or 1-octadecene). Products isolated

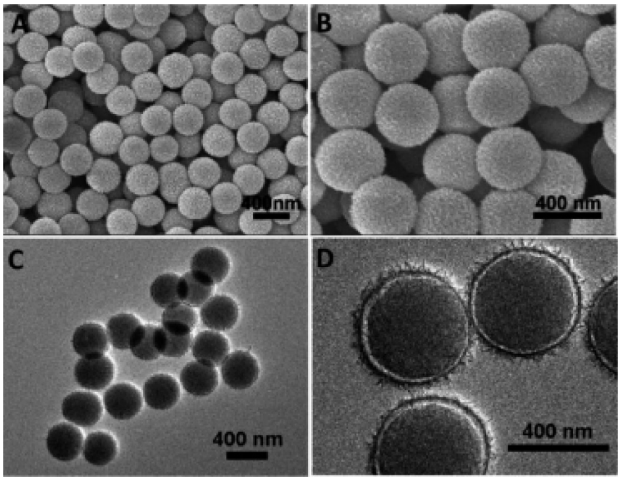

Figure 3. (A, B) SEM images and (C, D) TEM images of core−shell structured SiO_2 @nickel silicate nanospheres. [Reprinted from ref 41 with permission from Royal Society of Chemistry].

dx.doi.org/10.1021/cm401366q | *Chem. Mater.* 2013, 25, 3551−3569

are ~100 nm long Ni_9S_8 nanorods and ~50 nm irregularly shaped NiS particles.

Copper Sulfide. Copper sulfide (CuS) is a p-type semiconductor with a direct band gap of 1.2 eV−2.0 eV. Copper and sulfur are less toxic and relatively abundant. Copper sulfide is known to have at least fourteen different identifiable phases. Identified phases of copper sulfide include the following: chalcocite (Cu_2S), djurleite ($Cu_{31}S_{16}$or $Cu_{1.94}S$), digenite (Cu_9S_5 or $Cu_{1.8}S$), roxbyite (Cu_7S_4 or $Cu_{1.75}S$), covellite (CuS), and villamaninite (CuS_2).[44]

Over the past decade, copper sulfide nanoparticle synthesis has seen significant progress. Several methods have yielded nanoparticles with various shapes and that exhibit different properties. Structurally different copper sulfide nanoparticles were obtained using an amine-assisted hydrothermal process wherein variation of linking agents such as triethylenediamine, trimethylethylenediamine, and di-*n*-butylamine gave rise to nanowirelike aggregates (120 nm diameter and 2 μm length), nanotubelike aggregates (40−200 nm diameter and 400 nm−20 μm length), and nanovesicle-like aggregates (50−180 nm). The method gives variation in structural orientation by changing the linking agent and occurs in a single step simple process.[45] Similar hydrothermal conditions (~130 °C) applied to a microemulsion containing CTAB/*n*-$C_5H_{11}OH$/n-C_6H_{14}/water yielded distinct CuS flakes and addition of *n*-dodecanethiol to the microemulsion gave smaller hexagonal Cu_2S nanodisks.[46] A solventless approach to synthesize copper sulfide nanorods has been reported from a thiolate-derived precursor. The precursor was generated by combining a $Cu(NO_3)_2$ solution with chloroform and sodium octanoate (a phase transfer catalyst). The resulting blue copper octanoate complexes were added to dodecanethiol, and the solvent was evaporated to obtain a waxy residue, which was then dried at 148 °C for 140 min, redispersed in chloroform, and precipitated in ethanol. The nanorods obtained at 148 °C were 4 nm in diameter and 12 nm in length.[47]

Copper sulfide nanorods were also synthesized on molecular templates. Arachidic acid assembles on graphite as 1D nanostripes which were exploited and analyzed in atomic force microscopy. Copper arachidate films are obtained as curved stripes, and on reaction with hydrogen sulfide a straight orientation was regained. This method also has potential use for fabricating nanorod array based semiconductor materials.[48] Growth of ultrathin nanowires of Cu_2S was achieved by the use of a binary surfactant solvent. The ultrathin nanowires were obtained by treating $CuCl_2{\cdot}2H_2O$, dodecanethiol, and oleic acid (1/3, v/v) and the addition of sodium diethyl dithiocarbamate. Varying the volume ratios dithiocarbamate (DT) to oleylamine (OA) has an effect on the nanoparticles size and shape. Optical studies suggest the nanowires, 2.5 and 1.7 nm in diameter, exhibit high aspect ratio. The estimated band gap energies are in the range of 3.47 to 3.69 eV, leading to stronger quantum size effect; hence, they show high potential for use in photovoltaic applications.[49] Zhang et al. produced β-Cu_2S hexagonal nanoplates at high temperature (200−230 °C) in a solution-phase method using copper acetylacetone, elemental sulfur, and oleylamine which self-assembled closely into three-dimensional superlattices, enabling use in solar cell and semiconductor applications.[50] In a similar solution-phase method, copper acetylacetonate dissolved in dichlorobenzene and elemental sulfur were refluxed at 182 °C.[51] The copper sulfide nanocrystals obtained were hexagonal CuS (covellite) and rhombohedral $Cu_{1.8}S$ (digenite) depending on the Cu:S ratio. Hexagonal nanodisks in solution formed and assembled as stacked ribbons on a TEM grid.

The sacrificial templating method is another approach that has been investigated for the synthesis of nanoparticles. Wu et al. synthesized uniform CuS nanotubes by using copper nanowire precursors as sacrificial templates.[52] This approach involves the addition of an aqueous solution of 0.1 M $Cu(NO_3)_2$ to a homogeneous solution of NaOH in distilled water followed by addition of ethylene diamine and hydrazine. After mixing for 2 h at 60 °C copper nanowires were obtained, which were sonicated with ethylene glycol and thiourea and incubated at 80 °C for 12 h. The solid product was collected and washed with absolute ethanol and vacuum-dried at 60 °C. Characterization by XRD, TEM, and FESEM reveals the product to be hexagonal CuS nanotubes of 20 nm−50 nm inner diameter and 120−150 nm outer diameter, respectively. Another attempt at crystal templating was carried out using shape-controlled Cu_2O crystals, in which Cu_2O crystals with various morphologies (cubic, octahedral, and starlike shapes) have been employed as the template for obtaining the respectively shaped Cu_xS mesocages. The Cu_xS mesocages are produced by treating the Cu_2O crystals in Na_2S aqueous solution and dissolution of the Cu_2O inner core in a solution of ammonia.[53] Figure 4 shows SEM images of the Cu_xS mesocages.

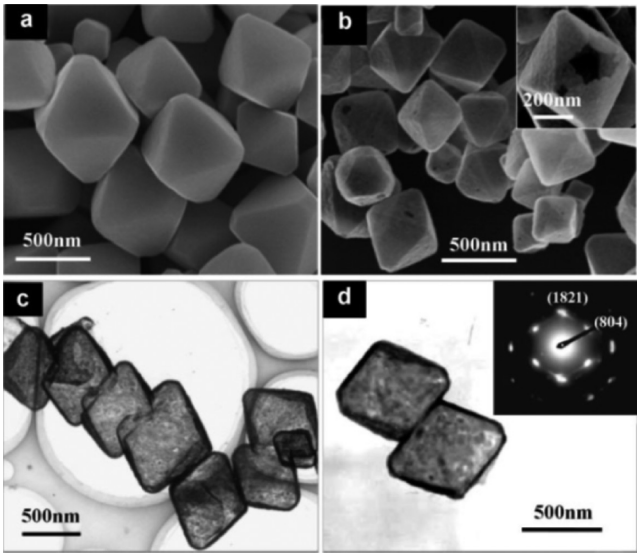

Figure 4. SEM images of a) octahedral Cu2O precursor crystals and b) octahedral Cu_xS cages. The inset of (b) shows an individual broken octahedral cage. c,d) TEM images of octahedral Cu_xS cages. The inset of (d): the SAED pattern of the upper octahedral cage. [Reprinted from ref 53 with permission from John Wiley and Sons].

Self-assembled single crystalline CuS (covellite) nanoplatelets about 26 nm in diameter and 8 nm thickness were synthesized by the solvothermal process using toluene as a solvent, hexadecylamine as the capping agent, and carbon disulfide and copper acetate as precursors.[54] The process gave single crystalline β-Cu_2S which was also grown in situ on multiwalled carbon nanotubes as spherical particles and triangular plates by varying precursor concentrations.[55] A soft template method was used to prepare hollow nanospheres of CuS with optical limiting properties suggesting the material is suitable for use in optical sensors and human eye protection

dx.doi.org/10.1021/cm401366q | *Chem. Mater.* 2013, 25, 3551−3569

devices. The material's optical limiting property is attributed to free carrier absorption and nonlinear scattering.[56] Single source precursors were used to synthesize faceted, hexagonal, closely packed CuS nanocrystals ~9.8 nm in triangular nanoplate form with six petal flowerlike shapes.[57] This method again shows control of the size and shapes of nanocrystals by varying a number of reaction parameters such as number of carbons in the substituted alkyl (n), reaction temperature, and precursor concentrations. Nanostructures from single source precursors have also been synthesized using L-cysteine.[58] Varying the L-cysteine to $CuCl_2 \cdot H_2O$ ratio gave rise to a variety of nanocrystals with snowflake, flower, and hollow spherelike structures. Single nanocrystalline hexagonal nanoplates of copper sulfide were also prepared by chemical vapor reaction, which grew perpendicular to the substrate surface.[59] Polydispersed $Cu_{2-x}S$ nanocrystals have been prepared using Cu-alkylamine with sulfur/1-dodecanethiol.[60] The dodecanethiol reduces sulfuration reaction temperature. In this work Cu defects detected by XPS are reported to arise due to introduction of S_2^{2-}, and this defect is claimed to be controlled by the right choice of Cu−alkylamine complexes. In situ source-template-interface reaction a wet chemical method has been used to synthesize one-dimensional CuS twinned nanorods at a low temperature of 105 °C as a variation to the common solvothermal attempts.[61] A simple solution phase thermolysis method was employed to develop Cu_2S nanocrystals and superlattices in the forms of monodispersed nanodisks, nanospheres, and nanoplates.[62] Nanoarrays of various shapes were prepared by altering the experimental conditions, and studying the self-assembly of the nanoparticles revealed some connection to the lamellar structure of the copper thiosulfate precursors.

An interesting synthesis of copper sulfide nanocrystallites was carried out by Tenhu et al.[63] The Cu_2S nanocrystallites were synthesized using 4-cyanopentanoic acid dithiobenzoate (CPAD) along with $CuCl_2$ in a 50/50 volume mixture of deionized water and ethanol and a solution of $NaBH_4$ in deionized water/ethanol under N_2 atmosphere. The nanocrystallites, sized around 1.4 nm, exhibit hexagonal phase at low temperatures and are transformed into the cubic phase $Cu_{1.8}S$ after considerable consolidation at temperatures of 100 to 240 °C. On sintering the nanocrystallites on paper at 240 °C, they showed no evident oxidative degradation and possessed high resistivity of the order of 1×10^{-5} ohm.[64] Self-assembled nanoribbons 30−70 nm in diameter were synthesized using hydrogel fibers from a derivative of L-glutamic acid.[65] Mineralization shows that the Cu ions were bound to the carboxylate ions on the surface, and infusion of H_2S enabled them to act as growth points for further growth. Thermal decomposition of CuSCN hollow spheres with ammonia (aqueous) at 450 °C yielded Cu_2S hollow nanospheres, and their characterization reveals an energy band gap of 2.96 eV.[66] Alivisatos et al. have made good quality Cu_2S nanocrystals by an injection reaction using copper(II) acetylacetonate and ammonium diethyl dithiocarbamate to synthesize the copper diethyldithiocarbate in situ in a solvent mixture of dodecanethiol and oleic acid.[67] The synthesized nanocrystals have also been used for fabricating photovoltaic devices with CdS (Figure 5) and show a power conversion efficiency of 1.6% on both glass and plastic substrates with lasting stability.

$Cu_{2-x}S$ nanocrystals were prepared by sonoelectrochemical, hydrothermal, and solventless thermolysis methods. The compositions of the nanocrystals varied from CuS (covellite)

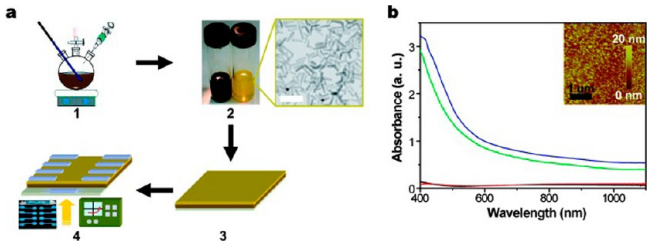

Figure 5. Fabrication and characterization of Cu_2S-CdS nanocrystals photovoltaic devices. (a) Scheme of Cu_2S-CdS nanocrystals photovoltaic device fabrication. (1) Solution-phase synthesis of Cu_2S nanocrystals and CdS nanorods. (2) Cu_2S nanocrystals and CdS nanorods are cleaned to make stock solutions for photovoltaic device fabrication. Inset, TEM image of CdS nanorods. The scale bar is 50 nm. (3) PEDOT:PSS, Cu_2S nanocrystals, and CdS nanorods are sequentially spin-cast onto ITO-coated glass substrates. (4) Al electrodes are thermally evaporated onto the substrates under high vacuum and electrical measurements are performed. Inset, photography of the Cu_2S-CdS nanocrystals photovoltaic device. (b) UV−vis spectra of ITO-coated glass substrate (black curve), ITO substrate with PEDOT:PSS layer (red curve), ITO substrate with PEDOT:PSS and Cu_2S layers (green curve), and final device (ITO substrate with PEDOT:PSS, Cu_2S, and CdS layers, blue curve). Inset, AFM image of the final device shows an overall roughness less than 4 nm. [Reprinted from ref 67 with permission from American Chemical Society].

to $Cu_{1.97}S$ (djurleite) by altering different parameters in each method. The comparison of their characteristic properties suggest that the copper deficient copper sulfide nanocrystals are more stable than Cu_2S.[68] Well-characterized, layered copper thiolate precursors were used to synthesize uniform Cu_2S nanodisks by a solventless thermolysis at ~200−220 °C in N_2 atmosphere.[69] The nanocrystals grow from small nanoparticles to nanodisks and faceted nanodisks along with the transformation from metastable orthorhombic to monoclinic Cu_2S and aggregation culminates in a crystallization process.

In another study Zhu et al. provide a detailed account of controlling CuS hollow spheres.[70] Aggregation of Cu_2O spheres were used as sacrificial templates to construct the copper sulfide nanoparticles. The study shows that loose aggregation of the sacrificial templates facilitates fast nanoparticle synthesis at low temperature and altering aggregation degree aids the formation of hollow nanospheres. Hollow spheres of copper sulfide have also been derived via Cu_2O nanoparticles, by reducing copper sulfate with ascorbic acid and sucrose solution at room temperature. Exploiting the Kirkendal effect, the Cu_2O sacrificial template yielded $Cu_2O/Cu_{7.2}S_4$ and $Cu_{7.2}S_4$ as intermediates and converted to CuS with a post-treatment with sodium citrate.[71] Cu_2S nanowires with length of many micrometers have been synthesized from elemental sulfur on carbon-coated copper grids. The nanowire growth periods of the nanowires were shown to be influenced by the particle size of the sulfur source, and the morphology variation is obtained by altering aging time.[72]

Thiolate-capped Cu_2S nanodisks were synthesized from copper nanoclusters that were encapsuled by a thiolate monolayer using the tendency of interparticle aggregative growth and interfacial carbon−sulfur cleavage.[73] The nanodisks varied from 3 to 35 nm in disk diameter and 3−6 nm in thickness, respectively. They also show 1D/2D ordering on self-assembly and have potential use in nanoelectronics, sensing, etc. CuS nanoplates were synthesized from a biphasic solution of copper(II) acetylacetonate complex in dichlro-

dx.doi.org/10.1021/cm401366q | Chem. Mater. 2013, 25, 3551−3569

methane and alkaline thioacetamide using a modified hydrothermal reaction. The CuS nanoplates were shown to have a band gap of 2.2 eV in ethanolic solution which aids the photocatalytic mineralization of a number of dyes such as malachite green, methyl red, methyl orange, and eosin.[74]

Copper sulfide hollow nanospheres have interesting synthetic routes. A microemulsion-template-interfacial-reaction route using copper naphthenate as metal precursor and thioacetamide as sulfide source is one of them.[75] The nanoparticles were formed at the oil/water solvent interface; therefore, regulating the interfacial reaction rate is vital to obtain hollow copper sulfide nanospheres. In this study the diameter of the hollow spheres were varied between 110 and 280 nm by changing the oil phase content from 0.5 to 1.5 mL also maintaining the crucial reaction temperature at 50 °C. CuS nanocrystals formed via a solvothermal process from copper acetate and sulfur chloride as precursors in 95% ethanol for 24 h at 160 °C.[76] The nanostructure was made of eight intersectant nanoflakes with a half hexagon shape. On varying reaction conditions, sphere-flowerlike and leaflike shapes were also obtained. These as-prepared nanoparticles show high electrocatalytic activity toward methyl orange when compared to CuS nanoparticles of other shapes and can be successfully used as a methyl orange sensor. *á*-Chalcocite (Cu_2S), djurleite, and digenite were synthesized to study the phase transformation of *á*-chalcocite to copper deficient djurleite.[77] Studies show that while a chalcocite is less stable than djurleite, addition of excess copper can reduce the transformation rate and could aid in curbing the undesirable conversion.

A facile one-pot synthesis of copper sulfide heteronanostructures was carried out, eliminating the need for preparation and purification of nanoparticles separately to initiate growth of new ones.[78] Cu_2S–metal chalcogenide heteronanostructures such as Cu_2S–ZnS, Cu_2S–CuInS2, and Cu_2S–CuInZnS have been synthesized using noncoordinating 1-octadecene as the solvent. This method can be extended to other ternary and quaternary metal chalcogenide systems. Cu_2S was prepared by dissociating $[Cu(tu)_3]Cl$ in ethylenediamine and subjecting it to controlled chemical oxidation by iodine $Cu_{2-x}S$ (x = 0.2, 025, 0.88, and 1.00) at room temperature, which can be utilized as a simple but promising approach for developing various other nonstoichiometric compositions of copper sulfide systems and other copper chalcogenides.[79] Structural transformation of Cu(I)S nanorods has been investigated based on temperature induced size dependent solid–solid phase transition.[80] The study shows that when transition temperatures are reduced, high chalcocite phase appears in the smallest nanocrystals at low temperatures. The size dependence in phase transformation also suggests that obtaining morphologies that are not present in bulk materials at ambient temperatures may become feasible and can be useful in many applications. Monoclinic and tetragonal chalcocite nanoparticles were synthesized by varying amounts of iron added to the reaction mixture.[81] These two nanoparticles are useful in photovoltaic applications.

Using a CuO template, solvent controlled construction of polyhedral copper sulfides (Cu_7S_4, CuS) with various stoichiometries and microstructures have been achieved based on their intrinsic difference and surface states. The formed Cu_7S_4 microcages exhibit high photocatalytic activity, which promotes degradation of methylene blue. This may be a consequence of their nanotwinned building blocks. This study helps to understand the importance of nanotwinned structures and their potential applications.[82] Water-soluble CuS nanoparticles have been synthesized using a simple colloidal route with alanine.[83] Serial ion exchange has been used to prepare multishelled hollow Cu_2S nanospheres from Cu_2O.[84] The sulfide ions diffuse onto the Cu_2O surface and Cu^+ cations migrate from the Cu_2O bulk facilitating the Cu_2O/Cu_2S interface. This exchange is favored due to the comparatively low K_{sp} of Cu_2S than that of Cu_2O.

Recently, we have used the copper(II) complex of 1,1,5,5-tetraisopropyl-2-thiobiuret $[Cu(SON(CN^iPr_2)_2)_2]$ as a single source precursor for the preparation of copper sulfide nanoparticles by solution thermolysis.[85] The nanoparticles synthesized had various morphologies including spherical, hexagonal disks, and trigonal crystallites; depending on the reaction temperature, concentration of the precursor, and the growth time. Thermolysis experiments in oleylamine produced Cu_7S_4 nanoparticles as a mixture of roxbyite (monoclinic) and anilite (orthorhombic) phases. Pure anilite Cu_7S_4 nanoparticles were obtained when a solution of precursor in octadecene was injected into hot oleylamine, whereas djurleite $Cu_{1.94}S$ nanoparticles were obtained when a solution of the precursor in oleylamine was injected into hot dodecanethiol. The optical properties of the pure anilite Cu_7S_4 phase and the djurleite $Cu_{1.94}S$ are consistent with indirect band gap materials

Cadmium Telluride. Aqueous and organometallic routes have been the principal synthetic routes to functionalized CdTe. There have also been reports of CdTe nanoparticles grown by physical methods such as laser ablation and mechanical alloying.[86,87] The pioneering work by Bawendi et al.[88] described the organometallic route to CdTe by thermolyzing a metal alkyl and tri-*n*-octylphosphine telluride in tri-*n*-octylphoshine oxide. Slow growth and annealing in the coordinating solvent results in uniform surface and regular core structure. Talapin et al. modified this route by reacting dimethylcadmium with different tellurium sources in mixtures of dodecylamine and trioctylphosphine.[89] The CdTe particles obtained were highly luminescent with their emission colors covering the visible spectral range from green to red. The drawback of these routes is the use of extremely pyrophoric, unstable compounds such as dimethyl cadmium at high temperatures.

Peng reported a greener route to cadmium chalcogenide nanoparticles, which replaces the dimethylcadmium with cadmium oxide.[90] The route has been reported to be reproducible involving mild and simple reaction conditions and could have the potential for scaled up industrial applications. Kumar and Nann used a similar organometallic procedure, whereby cadmium stearate was reacted with trioctylphosphine telluride at 220 °C to give CdTe nanoparticles in the form of spheres, rods, and spikes.[91] The shape control of CdTe was eloquently shown by Colvin et al.[92] The controlled growth of CdTe was achieved via the pyrolysis of CdO and $Cd(O_2CCH_3)_2$ at a specific Cd to E mole ratio. TOPO was used as the coordinating solvent, and tetradecylphosphonic acid (TDPA) was also added to facilitate the anisotropic growth. The tetrapod morphology of CdTe was observed for the first time. The shape evolution of CdTe nanoparticles was also demonstrated by Revaprasadu et al.[93] who recently synthesized CdTe by a method previously reported for PbTe.[94] An aqueous suspension or solution of a cadmium salt (chloride, acetate, nitrate, or carbonate) was added to a freshly prepared NaHTe solution. The isolated bulk CdTe was then dispersed in trioctylphosphine (TOP) and

dx.doi.org/10.1021/cm401366q | Chem. Mater. 2013, 25, 3551–3569

injected into preheated HDA at temperatures of 190, 230, and 270 °C for 2 h. The as-prepared CdTe nanoparticles were then isolated by the addition of methanol, followed by centrifugation, and finally dissolution in toluene. The particle morphology varied with the use of different cadmium sources.

Korgel and co-workers reported the synthesis of rod-shaped CdTe by sequential precursor chalcogenide injection.[95] This approach facilitates separation of the nucleation and selective kinetically controlled epitaxial growth of the hexagonal [002] planes thereby forming rod-shaped CdTe particles. Green and Taniguchi showed that the structure of CdTe nanoparticles could be changed by adding a metal cation with a positive redox potential.[96] The evolution of CdTe from nanorods to branched structures was reported by Janssen et al.[97] They used a cadmium cluster compound, $Li_2[Cd_4(SPh)_{10}]$, as the single molecule precursor. Chikan et al.[98] reported the growth of CdTe nanoparticles in the presence of HDA, HPA, and TOPO. The crystal growth of the particles was monitored by in situ UV−vis absorption spectroscopy which showed multiple excitonic peaks corresponding to various sizes of particles. They suggested that the 1.9 nm magic-sized CdTe, first observed in the reaction, aggregate to form larger particles.

The direct synthesis of CdTe nanocrystals in a poly(3-hexylthiophene) (P_3HT) matrix without the use of any surfactant was recently reported.[99] This in situ synthesis of nanoparticles in polymer matrix apparently improves the polymer−nanoparticles interface, which facilitates efficient electronic interaction between them. Spectral results suggest that CdTe nanocrystals are bound with P_3HT via dipole−dipole interaction and form a charge transfer complex. Structural and morphological studies reveal that CdTe works as a transport medium along/between the polymer chains, which facilitate percolation pathways for charge transport. Another hybrid structure, dumbbell-like CdTe/Au, was synthesized by the assembly of CdTe quantum dots with the assistance of $AuCl_4$ in aqueous solution.[100] The effect of $HAuCl_4$ concentration on the morphology of the products was also investigated. The morphology of the products evolved from sheaflike nanostructures to rodlike nanostructures and finally dumbbell-like nanostructures as the $HAuCl_4$ concentration was increased.

CdTe nanoparticles were grown from Te nanorods with the assistance of EDTA under hydrothermal conditions.[101] The experimental results showed that at the beginning of the reaction Te nucleated and grew into nanorods. As the reaction proceeds the CdTe nucleus began to emerge on the tips of the nanorods. Finally hexagonal CdTe nanoparticles with diameters of about 200 nm were obtained. Kolny-Olesiak et al. described the catalyst-free synthesis of CdTe nanowires in oleylamine.[102] Nanowires with cubic crystallographic structure and morphologies like ultrathin, straight, sawtoothlike, and branched could be synthesized using their method. The oleylamine reacts with cadmium acetate, activating the cadmium precursor resulting in a solution with a higher chemical potential. This process provides reaction conditions suitable for the formation of elongated structures through the oriented attachment mechanism.

An alternative to the organometallic route is the synthesis of water-soluble, thiol-stabilized CdTe nanoparticles.[103−105] This route is generally simple and cheap, and the particles have higher quantum yields than the organically passivated particles. Recently one-dimensional CdTe nanoparticles were synthesized by an ambient pressure aqueous solution method employing inorganic precursors and L-cysteine as the stabilizing agent.[106] Nanowires of CdTe formed through the spontaneous rearrangement of nanoparticles were reported by Kotov et al.[107] The self-assembly of the particles occurs when the organic stabilizer was removed, allowing the dipole−dipole interactions to drive self-organization. Weller pioneered the use of aqueous-based, thiol capped semiconductor nanoparticles. For CdTe, the synthesis utilized H_2Te as the tellurium source.[108] The highly flammable and toxic nature of tellurium gas resulted in the search for alternative tellurium sources. NaHTe and Na_2TeO_3 have been employed as sources of tellurium.[109,110] Gao et al. synthesized highly fluorescent CdTe nanoparticles using mercapto acids as the stabilizing agent.[111] Thioglycolic acid (TGA) and mercaptopropionic acid (MPA) gave the highest fluorescence. Green et al. used $(NH_4)_2Te$ to generate water-soluble CdTe which was then used in a biological imaging application.[112]

Alivisatos and co-workers were the first to exploit the properties of semiconductor nanoparticles in solar cell devices by using additional chemical and thermal treatment steps.[113] The inorganic nanocrystals, CdTe and CdSe were spin-cast from solution on indium tin oxide (ITO) glass coated with alumina. The CdTe film was first deposited followed by an annealing process and subsequent deposition of CdSe. High quality bilayer structures were formed with minimal intermixing at the surface. The initial studies showed power conversion efficiencies close to 3%. Olson and co-workers adapted this approach to show that colloidal CdTe nanorods can be used to fabricate single layered, sintered inorganic Schottky solar cells.[114] The Mulvaney group developed this method further by preparing $CdSe_xTe_{1-x}$ alloys through the sintering of thin films containing mixtures of CdTe And CdSe nanocrystals.[115] The optical bandgap can be tuned as a function of alloy composition. By using layer-by-layer assembly the films were incorporated into sintered photovoltaic devices with efficiencies up to 7.1%. They used the same approach to fabricate CdTe/ZnO thin-film solar cells.[116] ZnO was chosen as it readily converted to an n-type on exposure to UV, forming a p-n heterojunction when paired with CdTe. Through their approach chemical and thermal treatment between layers induce large scale grain formation resulting in the conversion of the 4 nm CdTe particles into films with an average crystallite size of ca. 70 nm.

Tin Sulfide. Tin sulfide is a IV−VI semiconductor and exists in three main forms including SnS, SnS_2, and Sn_2S_3.[117] It has attracted particular attention as a low-toxicity solar energy absorber,[118,119] in holographic recording[120,121] and for infrared detection. The band gaps of SnS, SnS_2, and Sn_2S_3 are 1.3 eV, 2.18, and 0.95 eV, respectively.[122−124] All three forms of tin sulfides exhibit the semiconducting properties; however, SnS has attracted the most attention due to its electronic bandgap which lies midway between those of silicon and GaAs.[125] It has been reported that depending on the tin content, SnS may be a p-type or n-type and also change its conductivity upon heat treatment.[126] SnS_2 is an n-type semiconductor, and Sn_2S_3 has highly anisotropic conduction.

There have been several routes employed to synthesize tin sulfide nanostructures. Hickey et al. synthesized SnS nanocrystals by the hot injection of thioacetamide in oleylamine into a mixture $Sn[N(SiMe_3)_2]_2$, oleic acid, trioctylphosphine, and octadecene.[127] The oleic acid/oleylamine ratio was varied to engineer the shape control of the particles. Liu et al. used a similar route to synthesize SnS, by injecting a solution of

dx.doi.org/10.1021/cm401366q | Chem. Mater. 2013, 25, 3551−3569

$S(SiMe_3)_2$ in octadecene into a solution of $SnCl_2$ in oleylamine at 200 °C.[128] The particle size was controlled by varying the reaction temperature; at all temperatures the orthorhombic phase was obtained. Recently Ning et al. synthesized SnS by dissolving $Sn_6O_4(OH)_4$ in oleic acid and oleylamine followed by the injection of thioacetamide with oleylamine at elevated temperatures ranging from 120 to 150 °C.[129] Xu et al. synthesized SnS nanocrystals by reacting $SnBr_2$ with Na_2S in ethylene glycol at room temperature in the presence of various stabilizing ethanolamines such as triethanolamine (TEA), N-methyldiethanolamine (MDEA), and N,N-dimethylethanolamine (DMEA).[130] The TEA capped SnS particles had an average size of 3.2 ± 0.5 nm, MDEA capped particles had an average size of 4.0 ± 2.0 nm, and the DMEA capped particles were 5.0 ± 4.0 nm in size.

Rectangular SnS nanosheets have been synthesized by pyrolyzing a single source precursor, $Sn(Dtc)_2(Phen)$ (Dtc = diethyldithiocarbamte, Phen = 1,10-phenanthroline).[131] Typical SEM and TEM images of the nanosheets are shown in Figure 6.

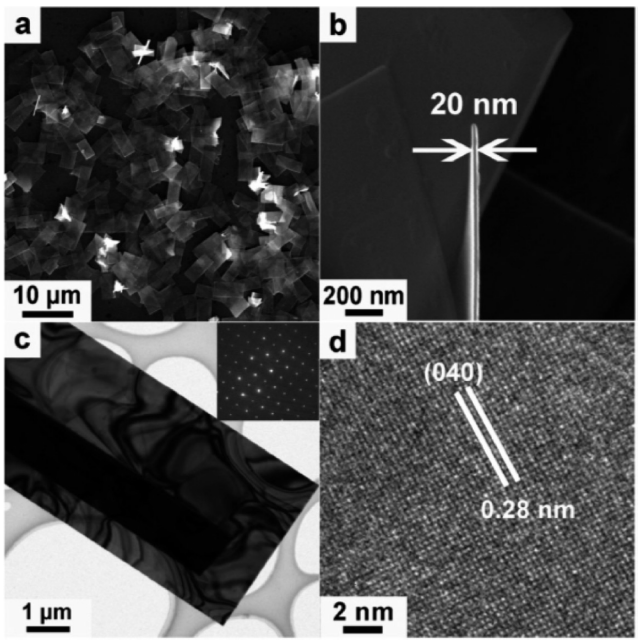

Figure 6. Typical SEM images (a) and (b), TEM and HRTEM images (c) and (d) of as-prepared SnS nanosheets. Inset in (c) is the SAED pattern of a nanosheet. [Reprinted from ref 131 with permission from Royal Society of Chemistry].

The SnS nanosheets were converted into nanoplates by changing the reaction conditions. The size and thickness of the SnS_2 nanoplates were about 150 and 6 nm, respectively. HRTEM and SAED analysis confirmed the crystalline nature of the nanoplates. A solvothermal route involving the reaction of tin dichloride ($SnCl_2 \cdot 2H_2O$) and potassium ethylxanthate ($C_2H_5OCS_2K$) in an autoclave at 180 °C produced SnS nanostructures in the form of nanosheets, nanoribbons, nanobelts, and nanorods.[132] The various morphologies of SnS were obtained by varying the reaction conditions such as reaction temperature, reaction time, and ratios of reactants. A slight excess of the ethylxanthate to tin chloride ratio resulted in the one-dimensional growth of lamellar SnS particles and their assembly into flowerlike superstructures.

Liu et al. reported the colloidal synthesis of size tunable SnS nanocrystals.[133] A sulfur-oleylamine precursor was injected into tin-oleylamine solution in the presence of hexamethyldisilazane (HMDS) at various reaction temperatures. The SnS particles in the 8−60 nm size range were close to spherical in shape, whereas the larger particles (ca. 700 nm) displayed unique crystal morphology. The direct band gaps of the different sized SnS nanocrystals ranged from 1.63 to 1.68 eV. The authors report that the particles have an unusual metastable cubic zinc-blende phase instead of the more stable orthorhombic phase. The phase change of SnS nanocrystals from orthorhombic to zinc-blende was also recently reported by Jin et al.[134] They employed a solution-based synthesis by thermolyzing tin(II) chloride and thioacetamide in diethylene glycol at reaction temperatures of 180−220 °C. Triethanolamine was added to the diethylene glycol reaction medium to control the growth of the particles. The influence of the triethanolamine addition in the diethylene glycol reaction medium, injection temperature and refluxing time on the crystal phase, growth morphology and optical properties of the SnS nanocrystals were investigated. The results showed that both the orthorhombic and zinc blende phase of SnS could be formed by altering the amount of triethanolamine. An earlier report by Greyson et al. also described the synthesis of SnS nanoparticles with a zinc blende crystal structure.[135] The SnS nano- and microcrystals were prepared by the reaction of $SnCl_2$ with elemental sulfur at 170 °C.

Nanocrystalline SnS_2 was prepared using organic stabilizers: cetyltrimethylammonium bromide (CTAB), sodium dodecyl sulfate (SDS), and p-benzenediarboxylic acid in ethanol.[136] By adjusting the type and concentration of the organic derivatives, SnS_2 nanostructures in the form of flowers, fibers, and sheets were obtained. Rajalakshmi et al. carried out optical and Raman scattering studies on SnS nanoparticles synthesized using a wet chemical method.[137] The Raman studies showed that all the predicted modes shift to lower wavenumbers in comparison to those of single crystals of SnS. This is attributed to phonon confinement.

Lead Sulfide. PbS has a narrow band gap of 0.41 eV. PbS is appealing because it exhibits strong quantum confinement effects due to the large Bohr radii of both electrons and holes. There have been many approaches to PbS nanoparticles with the chemical routes being favored over physical methods due to size and shape control that can be achieved during the synthesis procedure. It is important to achieve uniform size and shape to exploit the potential of nanoparticles with the desired properties.[138]

Hyeon and co-workers reported a similar general synthetic route for metal sulfide nanoparticles. The metal chloride is dissolved in oleylamine and reacted with an oleylamine solution of sulfur at 220 °C.[139] They have suggested that the reaction of sulfur with an amine gives an amine-sulfur compound containing a reactive Lewis basic sulfur group which is responsible for the high reactivity. Uniform cube-shaped PbS nanparticles with sizes of 6, 8, 9, and 13 nm were obtained. The Ozin group reported the synthesis of high quality PbS nanocrystals in multigram-scale quantities through a solventless, heterogeneous, and relatively greener route.[140] $PbCl_2$ and technical grade oleylamine were mixed and heated to 120 °C followed by the addition of a sulfur-oleylamine solution. The reaction is quenched by adding hexane, and the resultant solution is centrifuged to isolate the PbS nanoparticles. Photoluminescence studies on the particles show the particles to have a full width at half-maximum (fwhm) of 52 meV, a Stokes shift of 10 meV, and a quantum yield of 40%.

dx.doi.org/10.1021/cm401366q | Chem. Mater. 2013, 25, 3551−3569

Cao et al.[141] reported the synthesis of high quality PbS by reacting lead stearate and sulfur, stabilized by oleylamine in a noncoordinating solvent. The particles have strong absorption and photoluminescence emissions in the near-infrared region. Hines and Scholes reported a similar method by reacting lead oleate and bis(trimethylsilyl)sulfide (TMS). They reported the focusing of the particle size that occurred after the product was isolated from the reaction mixture. The particles displayed band gaps that were tunable across the near-infrared (NIR). The narrow shape of the emission spectrum and its position is an indication that the particles have a narrow size distribution, with the emission being primarily band edge (Figure 7).[142]

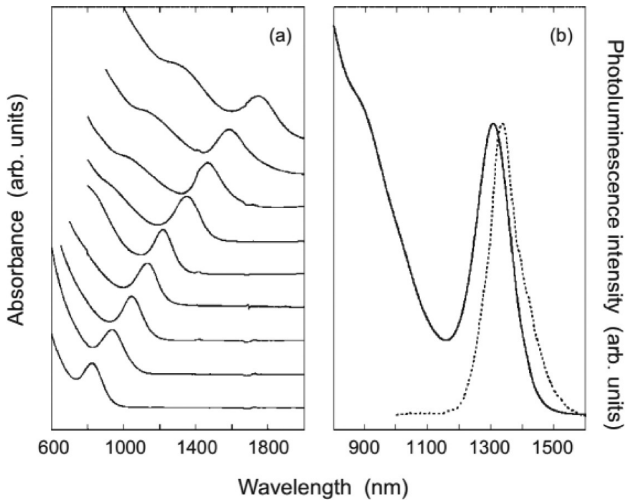

Figure 7. Room temperature optical characterization of toluene solutions of PbS nanocrystals. a) Absorption spectra spanning the range of tunable sizes. b) Band-edge and photoluminescence peaks for a sample ~6.5 nm in diameter. [Reprinted from ref 142 with permission from John Wiley and Sons].

Trindade and O'Brien reported the synthesis of lead(II) dithiocarbamato complexes $Pb(S_2CNRR')_2$ (R,R′ = Et, Bu, iBu) and their subsequent use as single source precursors for PbS nanoparticles.[143] The absence of the use of poisonous compounds such as H_2S or lead alkyls is a distinct advantage of this route compared to traditional organometallic routes. These compounds are stable for months and easy to synthesize and to thermolyze with high yields. The thermolysis of the $Pb(S_2CNEt_2)_2$ complex in tri-*n*-octylphosphine oxide (TOPO) gave cube-shaped particles. Cheon et al. used the same precursor to synthesize various rod-based structures such as highly faceted, star-shaped, truncated octahedrons and cubes (Figure 8).[144] By varying the ratio of dodecanethiol ligand to the Pb/S single source precursor, the shape can be tuned from spherical to cubic. O'Brien and co-workers subsequently revisited the use of the lead dithiocarbamato complexes as precursors for PbS.[145] They synthesized a series of symmetrical and unsymmetrical N′N-dialkyldithiocarbamatolead(II) complexes and thermolyzed them in oleylamine at temperatures of 60−80 °C. Spherical particles were obtained at reaction temperatures of 60 °C. An increase in the temperature to 80 °C produced cubic particles. Lower reaction temperatures were reported by the same group when olive oil was used as an organic capping group.[146] This method was reported to be environmentally friendly as the use of olive oil eliminates the

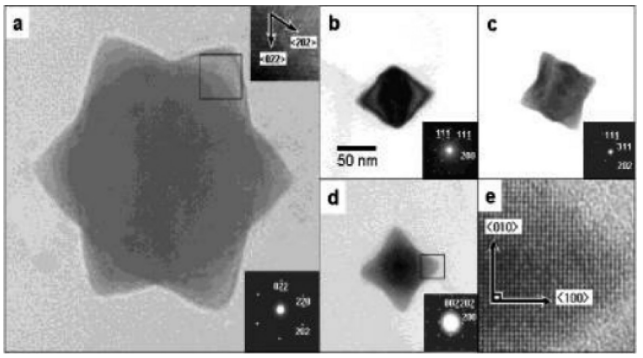

Figure 8. (a) TEM image of star-shaped PbS nanocrystals synthesized at 230 °C. (Inset) HRTEM imasge of lattice fringes with zone axis of [111]. (b-d) TEM images and electron diffraction patterns with zone axis of (b) [110], (c) [112], and (d) [100], respectively. (e) HRTEM image of zoomed fringes with zone axis of [100]. [Reprinted from ref 144 with permission from American Chemical Society].

use of air-sensitive, toxic, and expensive chemicals such as tri-*n*-octylphosphine and amines.

Another greener approach is the room temperature synthesis of PbS nanocubes by a solution based method in the presence of a sulfonated polymer.[147] Chen et al. reported the controlled synthesis of PbS via an environmentally friendly electrochemical route. They obtained PbS crystals with uniform size that show shape evolution from octahedral to starlike to football-like and finally to cubic morphology.[148] The evolution of shape is due to the variation of reaction parameters such as precursor concentration, deposition current, deposition time, and other relevant parameters of electrodeposition.

The use of heterocyclic lead dithiocarbamates was reported by the Revaprasadu group.[149] Lead piperidine dithiocarbamate (DTC) $[Pb(S_2CNC_5H_{10})_2]$ and lead tetrahydroisoquinoline dithiocarbamate $[Pb(S_2CNC_9H_{10})_2]$ were thermolyzed in hexadecylamine, dodecylamine, and decylamine to give PbS particles with varying shapes. The oleylamine capped PbS particles, synthesized using the lead tetrahydroisoquinoline dithiocarbamate complex, changed from cubes to rods on increasing the temperature from 180 to 270 °C. The decylamine-capped PbS particles synthesized from the lead piperidine dithiocarbamate complex were cubic or close to cubic in shape (Figure 9). Bis(thiosemicarbazide)lead(II) $[Pb(TSC)_2Cl_2]$ (TSC = thiosemicarbazide) was used to prepare star-shaped PbS nanostructures by a hydrolytic process.[150] The decomposition of a lead xanthate complex in ethylene diamine at room temperature produced cubes of PbS: another environmentally benign route.[151] Aromatic carboxylate complexes of Pb(II) that form stable adducts with thiourea or thiosemicarbazide were used as molecular precursors for PbS nanoparticles through decomposition in aqueous or non-aqueous solvents.[152] Depending upon reaction conditions truncated octahedra, dendrites, nanocubes, interlinked nanocubes, nanohexapods, and cubes were obtained. The authors studied the effect of single-source precursors on the mechanism of growth of nanoparticles, by comparing the decomposition results with PbS nanostructures synthesized from multiple-source precursors using lead acetate with thiourea or thiosemicarbazide. Growth from multiple source precursors appeared to happen faster than that from single-source precursors, although similar shapes were obtained for systems.

The growth of PbS nanorods is generally difficult because of its highly symmetric crystal structure. Warner demonstrated the

dx.doi.org/10.1021/cm401366q | *Chem. Mater.* 2013, 25, 3551−3569

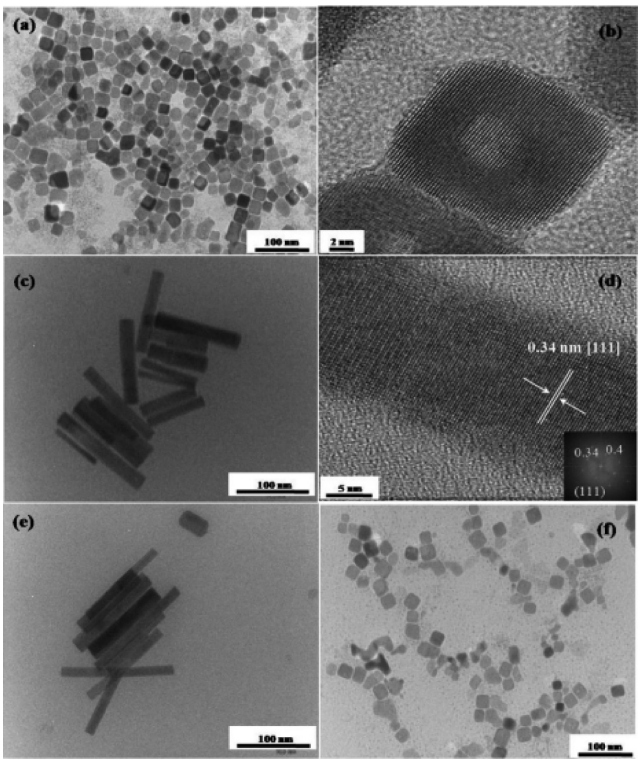

Figure 9. TEM and corresponding HRTEM images of OA capped PbS nanoparticles synthesized from the Pb(thq-dtc) complex at (a), (b) 180 °C, (c), (d) 2 h sample at 270 °C, (e) 4 h sample at 270 °C, and (f) from Pb(pip-dtc) at 230 °C. [Reprinted from ref 149 with permission from Royal Society of Chemistry].

use of combining multiple solvents such as oleylamine, oleic acid, and trioctylphosphine (TOP) to synthesize PbS particles ranging between cubes, stars, rods, and nanowires.[153] Each surfactant has a different functional group that reacts with the crystal facets of the PbS thereby controlling growth. When only oleylamine was used, regular cube-shaped particles were obtained. When two surfactants, e.g. oleylamine and trioctylphosphine, were used in combination, star-shaped particles were obtained after 5 min growth time. After 60 min the star-shaped particles evolved into rod-shaped structures. The rods had an average length of 44 nm and a breadth of 8.8 nm. When a third surfactant, oleic acid, was added, a branched network of nanowires was observed in the TEM images. Cloutier et al.[154] reported the synthesis of radically branched and zigzag nanowires through the self-attachment of star-shaped and octahedral nanocrystals via a hot injection route in the presence of multiple surfactants. Different surfactants may interact distinctly with the anions and cations, thus selectively coordinating with the different facets of the nanocrystals and modifying their surface energy during the reaction. After a considerable growth period the anisotropic growth will produce star-shaped and octahedral nanocrystals with a strong built-in dipole moment, which eventually becomes strong enough to generate the oriented attachment of the nanocrystals through dipole−dipole interactions. Through the mechanism of oriented attachment, branched and zigzag nanowires are formed.

Rod-shaped PbS was also synthesized by Revaprasadu and co-workers using a solution-based high temperature route.[155] Nanorods of PbS with varying lengths were formed when lead carbonate, nitrate, and sulfate were used as the lead sources. Solvothermal decomposition of lead dialkyldithiophosphate of the type $Pb[S_2P(OCnH_{2n+1})_2]_2$ (n = 4, 8, 12) in the presence of oleylamine 140−180 °C gave monodispersed cubic PbS particles.[156] The authors discussed in detail the systematic varying of the size and size distribution by adjusting reaction parameters such as reaction solvents, carbon number of the substitute alkyl, reaction temperature, and concentration of the single source precursors. Flowerlike PbS crystals were obtained through the microwave thermolysis of lead diethyldithiocarbamate.[157] Reports of using lead acetate and thiourea as lead and sulfur sources in microwave and ultrasonic irradiation have also been reported.[158] Very recently, Mighri et al. reported the synthesis of PbS from a methanolic lead acetate−thiourea complex via various precipitation techniques which included conventional chemical bath deposition, sonochemical, and microwave assisted chemical bath deposition.[159] The particles were capped by polyvinyl-pyrrolidone (PVP) and oleic acid.

Conventionally the colloidal route involves the precipitation of PbS by the reaction of a dissoluble lead salt and H_2S gas in an aqueous media. Organic[160−163] or inorganic[164,165] matrices have been used to stabilize the particles. The introduction of stabilizers has an influence on the chemical and physical properties of the particles. The embedding of PbS in polymers to form a nanocomposite structure has been extensively reported.[166−171] The growth of PbS in conducting polymers without surfactants allows effective charge transfer between the polymer and nanocrystal in photovoltaic devices.[166−169] Rodlike structures are preferred as they act as large surface area electron acceptors and provide continuous conduction pathways for electrons in a bulk heterojunction.

Recently a modified polyol process was used to prepare highly monodispersed, water-soluble PbS nanocrystals.[172] A thiourea stock solution was rapidly injected into the diethyene glyol solution containing a lead precursor and the capping group poly(acrylic acid), making the PbS water-dispersible. Biomolecules such as L-cysteine[173] were used with triethylamine[174] to produce water-soluble PbS nanoparticles. The L-cysteine was used as a sulfur source and chelating agent. Sheetlike PbS nanostructures were synthesized by a simple ethylenediamine-assisted hydrothermal method.[175] The ethylenediamine provides a weakly basic environment for the reaction system and also acts as a capping reagent to control the growth of cubic PbS. A hydrothermal method was also used to prepare single-crystal PbS using PEO−PPO−PEO triblock copolymer (P123) as a structure-directing agent.[176] SEM studies show that the nanorods have a diameter of 40−70 nm and a length of 200−600 nm, and both tips exhibit taperlike structures. A hydrothermal reaction between lead(II) salicylate and thiourea produced PbS nanostructures with varying morphologies.[177] The authors used the same method to synthesize PbS with a starlike morphology.[178] They reacted lead nitrate and thioglycolic acid (TGA) at relatively low temperature (80−160 °C) in an autoclave. The effects of the Pb^{2+} to TGA mole ratio in the starting solution on the morphology and shape of PbS was studied. The TGA acted as a 'soft template' leading to the anisotropic growth of PbS nanocrystals and forming starlike nanostructures. Another hydrothermal method described the synthesis of macrostarlike PbS hierarchical structures with the assistance of a new surfactant called tetrabutylammonium bromide (TBAB).[179] The mesostars were assembled from the PbS nanocube building blocks with edge lengths of about 100 nm. The authors provided a proposed mechanism for the formation of

dx.doi.org/10.1021/cm401366q | Chem. Mater. 2013, 25, 3551−3569

the mesostars. A soft hydrothermal route to PbS particles with diverse morphologies was reported by O'Brien and co-workers.[180] Air stable complexes, [2,2′-bipyridyl(Pb(SC(O)-$(C_6H_5)_2$)] and [$Pb(S_2(P(C_6H_5)_2)_2N)$], were mixed with thioglycerol and NaOH, and the resultant suspension was heated in a conventional pressure cooker at 100 °C. The variety of shapes achieved suggests that thioglycerol acts as a growth modifying agent.

Bismuth Sulfide. Bismuth sulfide (Bi_2S_3) is a direct band gap (1.3 eV) material with a potential of applications in solar cells. There has been growing interest in the preparation and application of bismuth sulfide nanostructures. A simple approach for the synthesis of snowflake and nanowires of Bi_2S_3 was reported using biomolecules, such as glutathione and lysozyme.[181,182] The representative synthesis involves microwave heating of $Bi(NO_3)_3$ with glutathione (GSH) in a Teflon vessel at 120 °C for snowflakelike structures. The flakelike structure was formed by assembly of 15 and 27 nm (dia) nanorods. Qian et al. reported the synthesis of Bi_2S_3 nanorods by a low-temperature solution method.[183] Nanorods were synthesized by the reaction of bismuth−thiolate complex and thioacetamide (TAA) in dodecanethiol at 95 °C. The nanorods synthesized by heating at 95 °C for 10 h were 18 nm in diameter and ∼200 nm in length. Yu et al. used ionic liquids for the synthesis of Bi_2S_3 nanostructures.[184] Bi_2S_3 nanostructures were prepared from $BiCl_3$ and thioacetamide and were kept with 1-butyl-3-methylimidazolium tetrafluoroborate ([BMIM]-$[BF_4]$) at 120 °C for 20 h. The isolated nanostructures were uniform nanoflowers (3−5 μm) composed of 60−80 nm (d) nanorods. Biomolecule-assisted synthesis was adopted for Bi_2S_3 nanostructures by Xie et al.[185] The hydrothermal reaction of $Bi(NO_3)_3{\cdot}5H_2O$ and L-cysteine in a Teflon-lined autoclave at 150 °C for 24 h produced a flowerlike structure of well aligned nanorods. A similar hydrothermal method using $Bi(NO_3)_3{\cdot}5H_2O$ and KSCN at 165 °C produced nanorods 20−40 nm in diameter and a few micrometers in length.[186] Ozin et al. reported the large scale (>17 g) synthesis of Bi_2S_3 ultrathin nanowires.[187] For the synthesis, sulfur in oleylamine was injected into a vessel containing bismuth citrate in oleylamine at 130 °C. This method gave ultrathin wires of Bi_2S_3 diameters <2 nm (Figure 10).

The Ozin group also studied the growth kinetics of nanowires and the surface and core structures at the cluster to nanocrystal transition.[188,189] Thermolysis of a bismuth−dithizone complex with acetylacetonate solution in an autoclave yielded Bi_2S_3 microspheres (5 μm).[190] The microspheres were composed of 20−40 nm nanorods. Thermolysis of bismuth complexes may have some advantages in terms of control over shape and size.

Bismuth complexes used for the synthesis of Bi_2S_3 nanostructures include bismuth(III) thioacetates [Bi-$(SCOPh)_3$],[191] pyridine and 1,10-phenanthroline adducts of bismuth(III) dithioxanthate complexes [$Bi(S_2COCH(CH_3)$-$CH_2CH_3)_3$],[192] bismuth(III) di-*n*-octyl-dithiophosphate [Bi-$(S_2P(OC_8H_{17})_2)_3$],[193,194] bismuth(III) diethyldithiocarbamate complexes,[195−197] bismuth(III) thiourea $[Bi_6(pydc)_8(Hpydc)_2(tu)_8]$, and bismuth(III) thiocarbazide $\{[Bi_2(pydc)_3(tsc)(H_2O)_2]{\cdot}H_2O\}_\infty$ complexes.[198] Most of these single source precursors produced nanorods or nanotubes with various lengths and diameters. Recently, very small nanocrystals (∼3 nm) of Bi_2S_3 were synthesized by reaction of bismuth oleate and thioacetamide in octadecene and oleic acid.[199] The nanocrystals showed a band gap around 1.5 eV and also exhibited a photoluminescence emission peak at 825 nm.

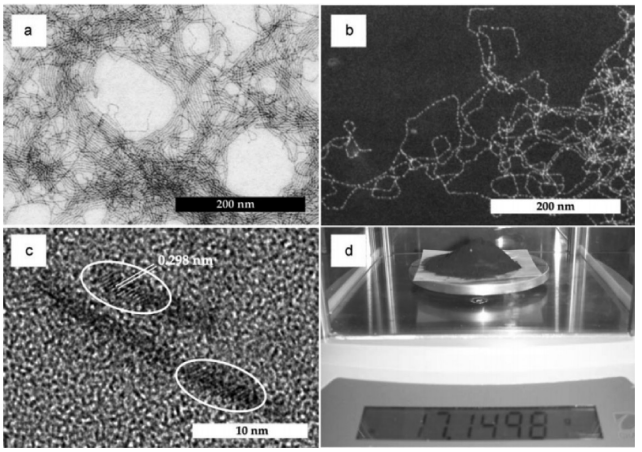

Figure 10. Microscopic characterization of Bi_2S_3 necklace nanowires. TEM (a) and ZC-TEM (b) of the Bi_2S_3 nanowires deposited on a carbon coated grid; c) HRTEM of nanowire fragments—the ellipses highlight the areas of the wire where the orientation of the crystalline lattice of the nanocrystals is parallel to the beam—the lattice spacing of 0.298 nm highlighted in the figure corresponds to (021) planes of the Bi_2S_3 structure; d) demonstration of ultralarge scale synthesis obtained from a ∼350 mL reaction: the wires depicted have been stripped off the ligand by hydrazine treatment [Reprinted from ref 187 with permission from John Wiley and Sons].

TERNARY AND QUATERNARY CHALCOGENIDES

Copper Indium and Copper Indium Gallium Chalcogenides. Copper indium sulfide and selenide are I−III−VI_2 ternary compound semiconductors absorbing in the red region of solar spectrum. These direct band gap ($CuInS_2$, 1.5 eV; $CuInSe_2$, 1.0 eV) semiconductor materials possess high optical coefficients, suitable for solar cells. $CuInS_2$ or $CuInSe_2$ is mainly used in thin film solar cell. These thin films are generally prepared by conventional growth methods such as sputtering, evaporation or chemical vapor deposition. The Korgel group introduced the concept of nanoinks for printable solar cells.[200] A facile method for size- and shape- controlled synthesis of $CuInS_2$ nanocrystals was carried out by thermolysis of Cu(OAc), $In(OAc)_3$ and dodecanethiol in 1-octadecene (ODE) at 240 °C.[201] $CuInS_2$ nanoparticles of 2 to ∼5 nm and nanorods with an aspect ratio of 1 to ∼3 were obtained by adjusting the reaction parameters such as temperature and time. The nanoparticle solutions showed a quantum confinement effect with tunable absorption (550−750 nm) and emission (600−750 nm) peaks. The lifetime of photoluminescence emission of the nanocrystals was investigated by the time-resolved photoluminescence decay technique. The decay curve of the $CuInS_2$ nanoparticles showed a triple exponential characteristic with lifetimes of 4−12, 28−60, and 140−300 ns corresponding to band exciton recombination, surface-related recombination, and donor−acceptor defects recombination of $CuInS_2$ nanocrystals.

Allen and Bawendi synthesized $CuInSe_2$ quantum dots with tunable emission between red and near-infrared.[202] Halides of copper and indium were heated with trioctylphosphine (TOP) and oleylamine to 280−360 °C. A solution of bis-(trimethylsilyl)selenide $[(Me_3Si)_2Se]$ in TOP was injected into a halides vessel and then the nanoparticles continued to

dx.doi.org/10.1021/cm401366q | Chem. Mater. 2013, 25, 3551−3569

grow at temperature between 200 and 280 °C. The $CuIn_5Se_8$ and $CuIn_{2.3}Se_4$ nanoparticles were reported to be 2−3.5 nm and 3−3.5 nm, respectively. The band gap of Cu−In−Se nanoparticles was varied from 1.3 eV (975 nm) to 1.94 eV (640 nm). The O'Brien group has synthesized $CuInSe_2$ nanoparticles by following a simple two step method.[203] In the first step, a mixture of CuCl and $InCl_3$ in trioctylphosphine was injected into trioctylphosphine oxide at 100 °C. Trioctylphosphine selenide (TOPSe) was injected at 250 °C. The absorption of as-isolated nanoparticles was obtained at 420 nm (2.95 eV) with a sharp excitonic peak at 352 nm. The photoluminescence spectrum showed emission at 440 nm. TEM showed spherical nanoparticles with size around 4.5 nm.

Chalcopyrite phase copper indium sulfide ($CuInS_2$) and copper indium gallium selenide ($Cu(In_xGa_{1-x})Se_2$; CIGS) nanocrystals were synthesized by arrested precipitation.[200] The synthesis of $CuInS_2$ nanoparticles from $Cu(acac)_2$ and $In(acac)_3$ in dichlorobenzene (DCB) with elemental sulfur at 182 °C was achieved. The nanoparticles were isolated by addition of ethanol into a reaction vessel. $CuInSe_2$ nanoparticles, CuCl, $InCl_3$ and elemental selenium were heated along with oleylamine to 240 °C for 4h. Chloroform was added to quench the reaction after cooling to ∼100 °C and then the nanoparticles were precipitated by adding ethanol. A similar process was followed for the synthesis of $CuInGaSe_2$ (CIGS) nanoparticles. The size of the nanoparticles was found to be 6−12 nm for $CuInS_2$ and 15 nm for $CuInSe_2$. The measured band gaps for $CuInS_2$ and $CuInSe_2$ nanoparticles are 1.29 and 0.95 eV, respectively. This nanoparticle solution was used as ink for the dip-coating or drop casting process. The photographs of nanoink and thin film preparation are shown in Figure 11. The solar cell device using $CuInSe_2$ nanoparticles has a Mo/$CuInSe_2$/CdS/ZnO/ITO configuration. The cell showed open circuit voltage of 300 mV with ∼3 mA cm^{-2} short circuit current density and a 0.25 fill factor. The efficiency was obtained as maximum of 0.2%. Pan et al. reported the first synthesis of cubic and wurtzite phase $CuInS_2$ nanoparticles.[204] For the synthesis of cubic phase $CuInS_2$, diethyl dithiocarbamate complexes of copper and indium were thermolyzed in a mixture of oleic acid and octadecene at 200 °C. The reaction was activated by injecting oleylamine. A similar process was carried out for the synthesis of wurtzite phase $CuInS_2$ nanoparticles, but with dodecanethiol as a capping agent.

Korgel et al. reported that the wurtzite phase of $CuInS_2$ can also be synthesized by reacting CuCl, $InCl_3$ and thiourea in oleylamine at 240 °C.[205] Monodispersed nanodisks of $CuInS_2$ were isolated with an average diameter and thickness of 13.4 and 5.7 nm. They found a considerable amount of chalcopyrite phase along with wurtzitic $CuInS_2$ based on the intensities of X-ray diffraction peaks. A high resolution transmission electron microscope investigation revealed that there is a coexistence of chalcopyrite and wurtzite phases within each nanodisk. Figure 12 shows HRTEM images and their corresponding FFT displaying explaining polytypism in a single nanodisk. Batabyal et al. thermolyzed the single source precursor $[(Ph_3P)CuIn(SC\{O\}Ph)_4]$ and dual source precursors $[Cu(SC\{O\}Ph]$, $[In(bipy)(SC\{O\}Ph)_3]$ in trioctylphosphine oxide (TOPO) and dodecanethiol (DT) to grow wurtzite and cubic phase $CuInS_2$ nanocrystals.[206] Kruszynska et al. reported the synthesis of Cu_2S-$CuInS_2$ hybrid and pure $CuInS_2$ nanostructures.[207] For the synthesis $CuInS_2$ nanocrystals, $Cu(OAc)$, $In(OAc)_3$ and trioctylphosphine oxide (TOPO) were mixed with oleylamine. A mixture of 1-dodecanethiol and *t*-dodecanethiol was injected into the vessel at 240 °C. The isolated nanoparticles were heterostructures of Cu_2S-$CuInS_2$. Cu_2S-$CuInS_2$ can be transformed into $CuInS_2$ by treatment with 1,10-phenanthroline at room temperature for 17 or 24 h. This method yielded wurtzite phase $CuInS_2$ nanostructures, as confirmed by Rietveld analysis.

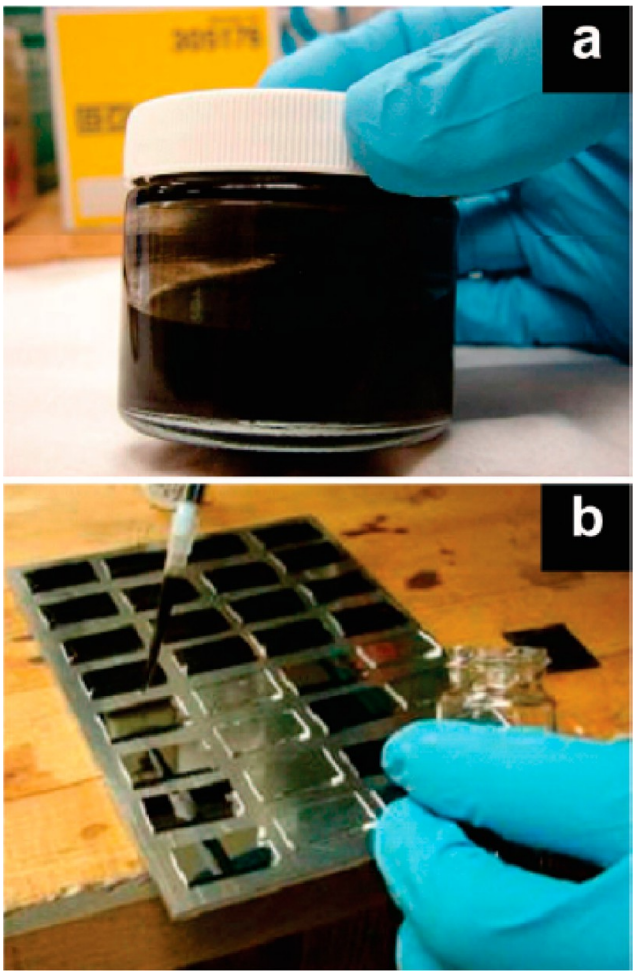

Figure 11. Photograph of (a) a $CuInSe_2$ nanocrystal dispersion and (b) the deposition of thin films on an array of glass substrates. After depositing the films, the substrates were placed in a vacuum oven at room temperature for 12 h [Reprinted from ref 200 with permission from American Chemical Society].

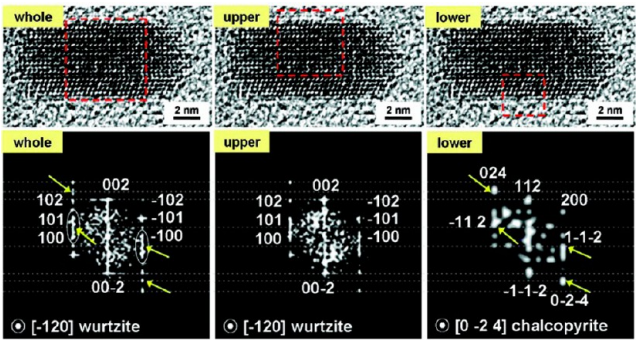

Figure 12. FFTs generated from a TEM image of a $CuInS_2$ nanodisk in the different regions of the crystal outlined in red. The additional spots in the FFT arise from the crystalline chalcopyrite domain ([0−24] zone axis), indicated by yellow arrows under the wurtzite domain [Reprinted from ref 205 with permission from American Chemical Society].

dx.doi.org/10.1021/cm401366q | *Chem. Mater.* 2013, 25, 3551−3569

The formation of Cu_2S-$CuInS_2$ hybrid nanostructures turned out to be an essential intermediate step in the growth of CIS nanoparticles. Copper sulfide played an important role in shape control of the CIS nanocrystals. $CuInS_2$ nanocrystals with a mean width of 19.1 ± 1.4 nm and a length of 44.8 ± nm $CuInS_2$ nanocrystals of elliptical shape were obtained by this method.

Ford et al. fabricated $CuIn(SSe)_2$ thin films by selenizing $CuInS_2$ nanocrystals.[208] $CuInS_2$ nanocrystals were synthesized using acetates, acetylacetonates, iodides, chlorides, and nitrates. The effect of different sources on electronic properties and solar cells performances were investigated. Solar cells from $CuInS_2$ nanocrystals, synthesized using different sources, had almost the same carrier concentrations (1016 to 1017 cm^{-3}). Solar cells fabricated using $CuInS_2$ nanocrystals synthesized using the acetylacetonates of copper and indium showed a slightly higher photoconversion efficiency of 5.45% others showed 4.81% for iodide, 5.04% for nitrate, 4.61% for acetates and 4.74% for chloride. Figure 13 show J-V characteristics of

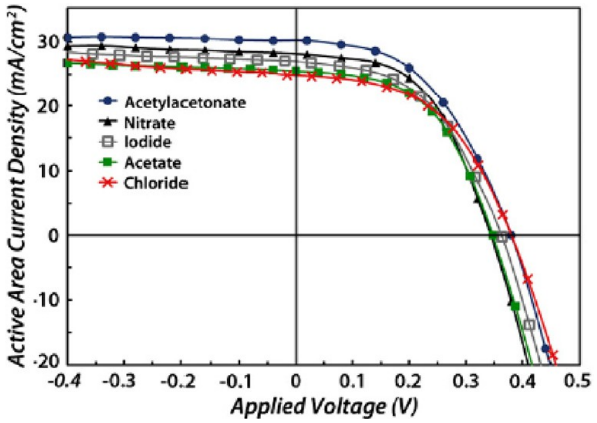

Figure 13. J–V characteristics of $CuIn(S,Se)_2$ devices under simulated AM1.5 G [Reprinted from ref 208 with permission from Elsevier].

$CuIn(SSe)_2$ devices prepared using different sources of copper and indium. Synthesis of $CuInS_2$ nanocrystals with strong visible to near-infrared photoluminescence was reported by Li et al.[209] $CuInS_2$ nanocrystals from copper iodide, indium acetate, and 1-dodecanethiol heated to 230 °C showed 5–10% photoluminescence quantum yield, which was further improved to over 80% after growing thin layer of ZnS or CdS on the $CuInS_2$ nanocrystals. Recently, $CuInS_2$ nanocrystals with photoluminescence quantum yields of 8.6–12.7% were reported.[210] Photoemission was tuned between red (623 nm), orange (598 nm) and yellow (564 nm) by varying the Cu/In ratio. By surface passivating these nanocrystals with ZnS, the quantum yield was improved to 68–78%. The authors showed that the combination of CIS/ZnS and a blue LED chip can be used as a blue-to-yellow wavelength converter. They also showed that a high luminous efficiency of 63.4 lm/W and a light conversion efficiency of 74.7% could be obtained at a forward current of 20 mA. Bao et al. reported a facile method for the synthesis of zinc-blende and wurtzitic $CuInS_2$ nanocrystals.[211] The synthesis of $CuInS_2$ nanocrystals is reported from a mixture of copper and indium oleate precursors injected into hot organic solutions of sulfur or dodecanethiol in oleylamine, octadecene, oleic acid. Anisotropic shapes in the form of triangular-pyramids, circular cones, and bulletlike rods were obtained by varying synthetic conditions such as the reactant concentration, the type of solvents, and the aging time. Zinc-blende or wurtzitic $CuInS_2$ nanocrystals can be prepared using elemental sulfur or Dod-SH as a sulfur source by systematically tuning reaction conditions, such as the reaction temperature and the concentration of the sulfur source.

Shen et al. reported the synthesis of copper indium selenide ($CuInSe_2$) nanocrystals with trigonal pyramidal shape via a two-step process.[212] The trigonal pyramid has edges 10–12 nm long. A hybrid solar cell based on the $P_3HT/CuInSe_2$ nanocrystals blends showed a promising open circuit voltage (V_{oc}) of 0.42 V and an energy conversion efficiency of 0.029% which is 3 times as that of the solar cell fabricated with only the naked P_3HT polymer. Recently, $[Sn(acac)_2Cl_2]$ was used as a capping agent for $CuInS_2$ nanocrystals.[213] The use of this complex improved the shape, size uniformity and also improved chemical composition and photoelectric response of $CuInS_2$ nanocrystals. In dodecanethiol $Cu(acac)_2$, $In(acac)_3$, and $Sn(acac)_2Cl_2$ were heated to 200 °C for 120 min. Copper, indium, and gallium complexes of diisopropyldiselenophosphinate were used for the synthesis of $CuInSe_2$, $CuGaSe_2$, and $CuIn_{1-x}Ga_xSe_2$ nanocrystals.[214] The compounds were thermally decomposed in hexadecylamine/trioctylphosphine oxide at 120–210 or 250 °C. The size of the nanoparticles could be varied by controlling the growth temperature, reaction time and precursor concentrations. Adjusting the precursor ratios and materials may lead to desired stoichiometric combinations.

Thermal decomposition of a mixture of copper $[Cu(SON(CN^iPr_2)_2)_2]$ and indium $[In(SON(CN^iPr_2)_2)_3]$ thiobiuret complexes yielded the chalcopyrite and wurtzite phases $CuInS_2$ nanocrystals.[215] Various shapes of nanoparticles such as spherical, hexagonal, trigonal, and conical were obtained. The solvothermal reaction of $CuCl_2$, $InCl_3 \cdot xH_2O$, and thioacetamide in oleylamine or ethylenediamine produced cubic and wurtzite phase $CuInS_2$ nanocrystals.[216] Cubic $CuInS_2$ nanocrystals were obtained when the reaction was carried out in oleylamine, whereas the wurtzite phase was obtained using ethylenediamine. Both phases of nanocrystals had particle size between 10 and 20 nm. Solar cells fabricated using these nanocrytstals spray-coated on Mo-coated sodalime glass showed a 0.78% photoconversion efficiency with an open circuit voltage of 0.13 and 0.19 V for wurtzite and cubic phase $CuInS_2$ nanocrystals, respectively. Guo et al. reported the fabrication of a thin film solar cell using $Cu(In_{1-x}Ga_x)S_2$ nanoink.[217] Nanocrystals ink was drop-casted onto Mo coated sodalime glass substrates. CIGSSe thin films were obtained by selenization of CIGS nanocrystals. The CIGSSe solar cell showed a 4.76% solar energy conversion efficiency with 455 mV of open circuit voltage and a 51.5% fill factor. A similar solar cell constructed using CISSe showed a 4.17% efficiency, a 393 mV open circuit voltage, and a 44% fill factor.

Recently, Lee et al. synthesized a large quantity of $CuIn_xGa_{1-x}Se_2$ and $CuIn_xGa_{1-x}S_2$ nanocrystals by a sonochemical method.[218] In this synthesis method, nanocrystals were synthesized without any capping agents or organic stabilizers which may act as an insulator in final solar cell. For the synthesis of CIGSSe nanocrystals, CuCl, $In(OAc)_3$, $Ga(NO_3)_3$, and Se/S were mixed with ethylene glycol and hydrazine monohydrate. The mixture was stirred in an ultrasonic generator for 3 h at 110 °C. Solar cells constructed using $Cu(InGa)Se_2$ nanocrystals showed an efficiency of 2.62%, an open circuit voltage of 305 mV, and a 49.7% fill factor. A $Cu(InGa)Se_2$ thin film solar cell was fabricated using

dx.doi.org/10.1021/cm401366q | Chem. Mater. 2013, 25, 3551–3569

nanoparticles precursors.[219] CIGS nanoparticles with size around 15 nm were prepared by a low-temperature colloidal route, in which CuI, InI_3, and GaI_3 in pyridine were reacted with Na_2Se in methanol at low-temperature. The nanoparticles are of the chalcopyrite phase with $CuIn_{0.71}Ga_{0.26}Se_{2.22}$ composition. The nanoparticle precursor was mixed with an organic binder and then coated on Mo-glass substrates by the doctor blade method. Resultant solar cells were 0.5% efficient, with a 220 mV open circuit voltage and a 31% fill factor.

The synthesis of wurtzite-structured $CuInGaS_2$ nanocrystals with controlled morphology and narrow size distribution has been reported.[220] $Cu(acac)_2$, $In(acac)_3$/$Ga(acac)_3$, and trioctylphosphine oxide (TOPO) were mixed with oleylamine (OLA) or octadecene (ODE). A mixture of 1-dodecanethiol and t-dodecanethiol was injected into a metal precursor vessel at 150 °C and maintained at 280 °C. CIS nanocrystals synthesized in OLA had a bulletlike shape with a uniform size of about 16 nm in width and 35 nm in length. Nanocrystals with a composition of $CuIn_{0.75}Ga_{0.25}S_2$ were rodlike with a shorter than average length. By replacing OLA with ODE as the solvent, the morphology of CIGS changes from bullet to nanorod, nanosphere, and nanotadpole shapes. CGS and $CuIn_{0.25}Ga_{0.75}S_2$ nanocrystals exhibited a tadpolelike shape, with the $CuIn_{0.25}Ga_{0.75}S_2$ nanotadpoles being relatively smaller in size. The band gap of the $CuIn_xGa_{1-x}S_2$ was increased from 1.53 eV for CIS to 2.48 eV for CGS. Recently, Jiang et al. reported a new method for the synthesis of $CuInSe_2$ and $CuIn_{1-x}Ga_xSe_2$ nanocrystals.[221] In their method of synthesis, metal chalcogenide complexes were used as surface ligands on the nanocrystals surface. The $CuInSe_2$, $Cu_{2-x}Se$ nanocrystals were capped with $In_2Se_4^{2-}$ or $CuInSe_2$ nanocrystals were capped with $\{In_2Cu_2Se_4S_3\}^{3-}$. It was reported that these metal chalcogenide complexes provide better colloidal stability and represent essential components of the target phase. Quaternary $CuIn_{1-x}Ga_x(S_ySe_{1-y})_2$ nanocrystals with an entire composition range have been synthesized; CuCl, $InCl_3$, $GaCl_3$, S, and Se were heated to 265 °C along with oleylamine.[222] The band gap of $CuIn_{1-x}Ga_x(S_ySe_{1-y})_2$ nanocrystals was tunable from 0.98 to 2.40 eV. All these $CuIn_{1-x}Ga_x(S_ySe_{1-y})_2$ nanocrystals were synthesized in the chalcopyrite phase. Solar cell fabricated using these nanocrystals showed a maximum photoconversion efficiency of 1.02% with an open circuit voltage of 260 mV and a 28% fill factor.

Solution–liquid–solid (SLS) is a method which utilizes catalysis for the growth of nanowires. A number of binary chalcogenide materials have been synthesized using this method. However, the SLS method has not seen much development for the growth of ternary chalcogenides. Recently, Hollingsworth and co-workers prepared $CuInSe_2$ nanowires by the solution–liquid–solid (SLS) mechanism employing both metal–organic multiple and single-source precursors.[223] The precursors were decomposed in molten metal (Au,Bi) nanoparticles and coordinating ligands. The single-molecule precursors readily gave high quality straight, crystalline, and close to stoichiometric $CuInSe_2$ nanowires. However the use of multiple precursors required careful fine-tuning of reaction conditions to obtain high quality $CuInSe_2$. They found that the choice of coordinating ligands, reaction temperature, and reactant order of addition had a profound influence on the morphology and composition of the final product.

Copper Zinc Tin Chalcogenides. Copper zinc tin sulfide (Cu_2ZnSnS_4; CZTS) is an emerging solar energy material. It has a band gap of ~1.5 eV with an absorption coefficient of 10^4 cm^{-1} and is composed of nontoxic and abundant elements. Due to its potential as an alternative material to CIGS in thin film solar cells, there has been considerable research focused on the synthesis and growth of CZTS nanocrystals and thin films in recent years. Solution processed CZTS-based absorber layers have shown the highest solar energy conversion efficiency (10.1%).[224] Recently, we have reviewed the synthesis and deposition methods for CZTS nanocrystals and thin films.[225] Here we review only the most recent progress on CZTS and its related materials.

Singh et al. synthesized wurtzitic CZTS with a nanorod morphology.[226] $Cu(acac)_2$, $Zn(OAc)_2$, $Sn(OAc)_4$, and TOPO were mixed with octadecene and heated to 150–160 °C. A mixture of 1-DDT and t-DDT was injected into the metal salts vessel at 150–160 °C, and the vessel continued to be heated to 240–260 °C. The as-synthesized nanorods had sizes of 35 ± 3 nm (l) and 11 ± 0.5 nm (d). In addition to the synthesis of nanorods, the authors also assembled the nanorods vertically on a TEM grid, and Figure 14 shows TEM and SEM images of nanorods assembly. Following this, Regulacio et al. developed a noninjection route for the synthesis of wurtzite phase CZTS nanocrystals.[227] In this work, diethyldithiocarbamate complexes of copper, zinc, and tin were decomposed in a mixture of hexadecanethiol and trioctylamine at 250 °C. The synthesized nanorods are nearly monodispersed with an average length and width of 15.1 ± 1 nm and 7.6 ± 0.6 nm, respectively. The authors described that the initially formed $Cu_{1.94}S$ nuclei facilitate the CZTS to grow as a wurtzitic phase. Recently, continuous production of CZTS nanocrystals in a flow reactor was developed.[228] Copper chloride, tin chloride, and zinc oxide were dissolved in oleylamine or octadecene and mixed with sulfur. Then the entire mixture was pumped through a meter long and 3 mm diameter bronze tube at 300–320 °C at a flow

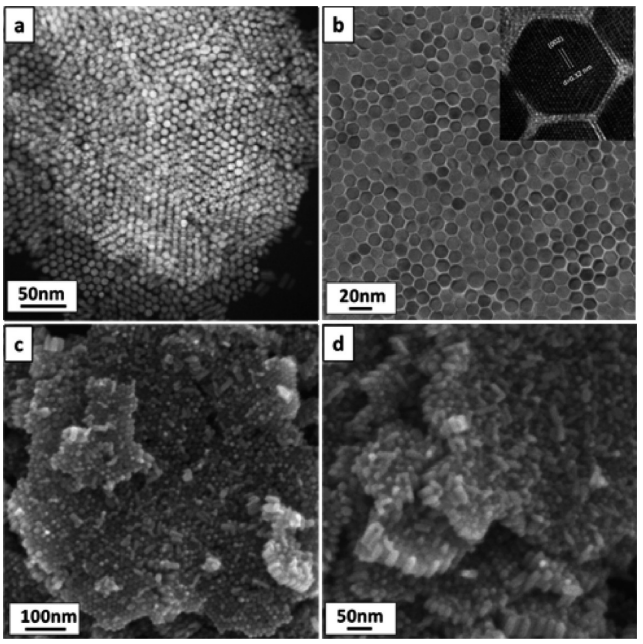

Figure 14. DF-STEM image shows 3D superstructure of CZTS nanorods. (b) Top-down HRTEM images show the closed-packed monolayer of CZTS nanorods with inset HRTEM image of single rod. (c) and (d) SEM and HRSEM images show the top-down and side view of multilayer assembly of CZTS nanorods [Reprinted from ref 226 with permission from American Chemical Society].

dx.doi.org/10.1021/cm401366q | Chem. Mater. 2013, 25, 3551–3569

rate of 1−5 mL/min. The as-synthesized nanocrystals had a fairly narrow size distribution; however, the full shape and size control is yet to be developed for this method.

CZTS nanocrystals with quantum confinement have been synthesized by the thermal decomposition method.[229] Diethyl dithiocarbamate complexes of copper, zinc, and tin were heated in oleic acid and octadecene, at temperatures of 150 °C (for 2 and 2.5 nm particles) and 175 °C (for 5 and 7 nm particles). Oleylamine and/or octadecene were injected into the reaction vessel to initiate the nanocrystals growth. The nanocrystals produced by this method are spherical with diameter of 2, 2.5, 5, and 7 nm. The quantum confinement effect in these nanocrystals was observed as an increase in band gap values from 1.5 to 1.8 eV upon reducing the particle size 7 to 2 nm. Riha et al. synthesized $Cu_2ZnSn(S_{1-x}Se_x)_4$ nanocrystals with a tunable composition and band gap.[230] The synthesis involve simultaneous injection of copper(II) acetylacetonate, zinc acetate, and tin acetate and a mixture of sulfur/selenium and $NaBH_4$ in oleylamine into the vessel containing trioctylphosphine oxide at 325 °C. The band gap of the nanocrystals decreased from 1.54 eV for $x = 0$ to 1.47 eV for $x = 1$. A similar approach was carried out for the synthesis of $Cu_2ZnSn(S_xSe_{1-x})_4$ nanocrystals by Ou et al.[231] A mixture containing stearate complexes of copper, zinc, and tin in oleylamine was injected into thiourea and elemental selenium in octadecene at 270 °C. Optical band gaps of $Cu_2ZnSn(S_xSe_{1-x})_4$ nanocrystals obtained by this method varied from 1.5 eV for $x = 1$ and 1.0 eV for $x = 0$. Nanowires and nanotubes of CZTS were synthesized on anodized alumina (AAO) template by a sol−gel method.[232]

A sol−gel CZTS was prepared by dissolving copper(II) acetate, zinc(II) acetate, and tin(II) chloride in 2-methoxyethanol. AAO templates with 200 nm pore size were immersed into CZTS precursor solution and then annealed at 550 °C under sulfur atmosphere. Both nanowires and nanotubes had a diameter around 200 nm and 60 μm lengths. CZTS nanowires and nanotubes showed optical band gaps of 1.57 and 1.61 eV, respectively. Tian et al. reported the preparation of CZTS nanocrystal-based ink and used it for the fabrication of a solar cell.[233] CZTS nanocrystals were synthesized by the solvothermal method, in which $CuCl_2 \cdot 2H_2O$, $ZnSO_4 \cdot 7H_2O$, and $SnCl_2 \cdot 2H_2O$ were added into ethylene glycol solution containing $Na_2S \cdot 9H_2O$. The whole mixture was transferred to a 30 mL autoclave and kept at 180 °C for 12 h. A solar cell fabricated on Al foil showed a 1.94% solar energy conversion efficiency, a 0.484 V open-circuit voltage, an 8.91 mA cm-2 short-circuit current density, and a 45.1% fill factor.

Recently, Saha et al. prepared a CZTS based hybrid *pn*-junction solar cell.[234] CZTS nanocrystals were synthesized by injecting $SnCl_4$ into a vessel containing $CuCl_2 \cdot 2H_2O$, $ZnCl_2 \cdot 2H_2O$, and sulfur in oleylamine at room temperature. Nanoparticle growth proceeded at 180 °C for 1 h. Nanoparticles were coated onto ITO substrate, and then [6,6]-phenyl-C61-butyric acid methyl ester (PCBM) was coated to form a hybrid structure. The hybrid solar cell showed a power conversion efficiency of 0.9% with a 43% fill factor. Jian et al. have isolated a metastable orthorhombic phase of Cu_2ZnSnS_4 nanocrystals.[235] The synthesis involves autoclaving $CuCl_2 \cdot 2H_2O$, $ZnCl_2$, $SnCl_2 \cdot 2H_2O$, and thiocarbamide in water and ethylenediamine at 200 °C for 24 h. The nanocrystals had a platelike morphology with sizes from 20 to 50 nm. The authors also reported that the metastable orthorhombic phase can be transformed to a stable kesterite phase by annealing at 500 °C

Shavel et al. reported the synthesis of $Cu_2ZnSnSe_4$ nanocrystals by the hot injection method.[236] Trioctylphosphine selenide (TOP-Se) was injected into a mixture containing CuCl, $ZnCl_2$, octadecene, and $SnCl_4$ at 295 °C. Isolated nanocrystals had polyhedral morphology with an average size of 20.0 ± 2 nm (Figure 15). Recently, a wurtzitic phase of

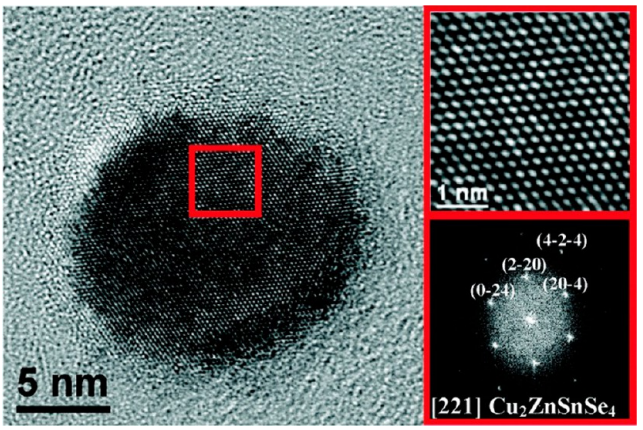

Figure 15. HRTEM micrograph of a CZTSe nanocrystal (left) with the fast Fourier transform pattern (bottom right) of the selected area of the same particle (top right). [Reprinted from ref 236 with permission from American Chemical Society].

$Cu_2ZnSnSe_4$ nanocrystals was synthesized by Wang et al.[237] The synthesis involves thermal decomposition of Cu-oleate, Zn-oleate, Sn(II) 2-ethylhexanoate, and diphenyl diselenide at 255 °C for 40 min. Isolated nancrystals by this method had nearly spherical morphology with an average diameter of 19.3 ± 2.3 nm. The optical band gap of $Cu_2ZnSnSe_4$ nanocrystals was found to be 1.46 eV. Recently, Liu et al. identified a phosphine-free selenium source for the synthesis of $Cu_2ZnSnSe_4$ nanocrystals.[238] Selenium dissolved in docecanethiol and oleylamine at room temperature was used as the selenium precursor and $CuCl_2$, $SnCl_4$, and $SnCl_4$ were heated with oleylamine and dodecanethiol to 180 °C. The Se-precursor was injected and maintained for 30 min. The as-synthesized nanocrystals were nearly monodispersed 3.4 nm spherical particles and showed an optical band gap of 1.7 eV.

■ CONCLUSION

The synthesis of nanostructured materials has seen tremendous advances during the past two decades with a variety of well-established protocols being reported. This review has highlighted some of the important developments in synthetic routes to materials which have applications in solar cells. The common routes to these materials include hydrothermal/solvothermal approaches, the use of dual or single molecule precursors via the 'hot' injection approach, and template directed routes. There are recent trends toward environmentally friendly methodologies using lower reaction temperatures such as electrochemical routes. All methods aim to control the size, shape, and surface properties of the nanostructured materials. The search for the new routes to synthesize nanomaterials will continue to yield high quality nanostructured materials with the desirable morphologies and properties that will ultimately lower the cost and increase the efficiency of solar cells. Despite the low-cost and easy processing, the performance of nanocrystal-

dx.doi.org/10.1021/cm401366q | *Chem. Mater.* 2013, 25, 3551−3569

line solar cell is yet to become viable. The major complications that restrict the performance of nanocrystalline solar cells are grain boundaries and surface defects. However, some progress has recently been made to address these issues.

AUTHOR INFORMATION

Corresponding Author

*E-mail: paul.obrien@manchester.ac.uk.

Notes

The authors declare no competing financial interest.

ACKNOWLEDGMENTS

K.R. is grateful to National Science Foundation under grant No. CHE 1012850. K.R. is thankful to Prof. Arunava Gupta. The authors also thank EPSRC, UK for the grants to P.O.B. that have made this research possible. N.R. would like to acknowledge the Department of Science and Technology (DST) and National Research Foundation (NRF), South Africa through the DST/NRF South African Research Chairs Initiative (SARCHi) program

REFERENCES

(1) Dhere, N. G. *Sol. Energy Mater. Sol. Cells* **2007**, *91*, 1376.
(2) Chapins, D. M.; Fuller, C. S.; Pearson, G. L. *J. Appl. Phys.* **1954**, *25*, 676.
(3) Zou, C.; Zhang, L. J.; Lin, D. S.; Yang, Y.; Li, Q.; Xu, X. J.; Chen, X.; Huang, S. M. *CrystEngComm* **2011**, *13*, 3310.
(4) Chen, G. Z.; Zhu, F. F.; Sun, X.; Sun, S. X.; Chen, R. P. *CrystEngComm* **2011**, *13*, 2904.
(5) Jager-Waldau, A. *Sol. Energy Mater. Sol. Cells* **2011**, *95*, 1509.
(6) Klenk, R.; Klaer, J.; Koble, C.; Mainz, R.; Merdes, S.; Rodriguez-Alvarez, H.; Scheer, R.; Schock, H. W. *Sol. Energy Mater. Sol. Cells* **2011**, *95*, 1441.
(7) Lai, C.-H.; Lu, M.-Y.; Chen, L.-J. *J. Mater. Chem.* **2012**, *22*, 19.
(8) Zhaoab, Y.; Burda, C. *Energy Environ. Sci.* **2012**, *5*, 5564.
(9) Rao, C. N. R.; Pisharody, K. P. R. *Prog. Solid State Chem.* **1975**, *10*, 207.
(10) Vaughan, D. J.; Craig, J. R. *Mineral Chemistry of Metal Sulfides*; Cambridge University Press: Cambridge, 1978.
(11) Nath, M.; Choudary, A.; Kundu, A.; Rao, C. N. R. *Adv. Mater.* **2003**, *15*, 2098.
(12) He, Z.; Yu, S.-H.; Zhou, X.; Li, X.; Qu, J. *Adv. Funct. Mater.* **2006**, *16*, 1105.
(13) Vanitha, P. V.; O'Brien, P. *J. Am. Chem. Soc.* **2008**, *130*, 17256.
(14) Han, W.; Gao, M. *Cryst. Growth Des.* **2008**, *8*, 1023.
(15) Min, Y.; Chen, Y.; Zhao, Y. *Solid State Sci.* **2009**, *11*, 451.
(16) Wadia, C.; Wu, Y.; Gul, S.; Volkman, S. K.; Guo, J.; Alivisatos, A. P. *Chem. Mater.* **2009**, *21*, 2568.
(17) Lin, Y. Y.; Wang, D. Y.; Yen, H.-C.; Chen, H. L.; Chen, C. C.; Chen, C. M.; Tang, C. Y.; Chen, C. W. *Nanotechnology* **2009**, *20*, 405207.
(18) Puthusery, J.; Seefeld, S.; Berry, N.; Gibbs, M.; Law, M. *J. Am. Chem. Soc.* **2011**, *133*, 716.
(19) Beal, J. H. L.; Etchegoin, P. G.; Tilley, R. D. *J. Phys. Chem. C* **2010**, *114*, 3817.
(20) Li, W.; Doblinger, M.; Vaneski, A.; Rogach, A. L.; Jackel, F.; Feldmann, J. *J. Mater. Chem.* **2011**, *21*, 17946.
(21) Bi, Y.; Yuan, Y.; Exstrom, C. L.; Darveau, S. A.; Huang, J. *Nano Lett.* **2011**, *11*, 4953.
(22) Beal, J. H. L.; Prabakar, S.; Gaston, N.; The, G. B.; Etchegoin, P. G.; Williams, G.; Tilley, R. D. *Chem. Mater.* **2011**, *23*, 2514.
(23) Akhtar, M.; Akhter, J.; Malik, M. A.; O'Brien, P.; Tuna, F.; Raftery, J.; Helliwell, M. *J. Mater. Chem.* **2011**, *21*, 9737.
(24) Paolella, A.; George, C.; Povia, M.; Zhang, Y.; Krahne, R.; Gich, M.; Genovese, L.; Falui, A.; Longobardi, M.; Guardia, P.; Pellegrino, T.; Manna, L. *Chem. Mater.* **2011**, *23*, 3762.
(25) Kirkeminde, A.; Ruzicka, B. A.; Wang, R.; Puna, S.; Zhao, H.; Ren, S. *ACS Appl. Mater. Interfaces* **2012**, *4*, 1174.
(26) Abdelhady, A. L.; Malik, M. A.; O'Brien, P.; Tuna, F. *J. Phys. Chem. C* **2012**, *116*, 2253.
(27) Acevedo, M. C.; Faber, M. S.; Tan, Y.; Hamer, R. J.; Jin, S. *Nano Lett.* **2012**, *12*, 1977.
(28) Macpherson, H. A.; Stoldt, C. R. *ACS Nano* **2012**, *6*, 8940.
(29) Manthiram, A.; Jeong, Y. U. *J. Solid State Chem.* **1999**, *147*, 679.
(30) Andersen, G.; Kofstad, P. *Oxid. Met.* **1995**, *43*, 173.
(31) Jarret, H. S.; Cloud, W. H.; Bouchard, R. J.; Butler, S. R.; Frederick, C. G.; Gillison, J. L. *Phys. Rev. Lett.* **1968**, *21*, 617.
(32) Mulmudi, H. M.; Batabyal, S. K.; Rao, M.; Pranhakar, R. R.; Mathews, N.; Lam, Y. M.; Mhaisalkar, S. G. *Phys. Chem. Chem. Phys.* **2011**, *13*, 19307.
(33) Wadia, C.; Alivisatos, A. P.; Kammen, D. M. *Environ. Sci. Technol.* **2009**, *43*, 2072.
(34) Chen, N.; Zhang, W.; Yu, W.; Qian, Y. *Mater. Lett.* **2002**, *55*, 230.
(35) Tilley, R. D.; Jefferson, D. A. *J. Phys. Chem. B* **2002**, *106*, 10895.
(36) Zhang, W.; Xu, L.; Tang, K.; Li, F.; Qian, Y. *Eur. J. Inorg. Chem.* **2005**, 653.
(37) Ghezelbash, A.; Sigman, M. B.; Korgel, B. A. *Nano Lett.* **2004**, *4*, 537.
(38) Ghezelbash, A.; Korgel, B. A. *Langmuir* **2005**, *21*, 9451.
(39) Zhou, W.; Chen, W.; Nai, J.; Yin, P.; Chen, C.; Guo, L. *Adv. Funct. Mater.* **2010**, *20*, 3678.
(40) Barry, L.; Holmes, J. D.; Otway, D. J.; Copley, M. P.; Kazakova, O.; Morris, M. A. *J. Phys.: Condens. Matter* **2010**, *22*, 076001.
(41) Zhu, T.; Wang, Z.; Ding, S.; Chen, J. S.; Lou, X. W. *RSC Adv.* **2011**, *1*, 397.
(42) Wang, Y.; Zhu, Q.; Tao, L.; Su, X. *J. Mater. Chem.* **2011**, *21*, 9248.
(43) Aso, K.; Kitaura, H.; Hayashi, A.; Tatsumisago, T. *J. Mater. Chem.* **2011**, *21*, 2987.
(44) Fleet, M. E. *Rev. Mineral. Geochem.* **2006**, *61*, 365.
(45) Lu, Q.; Gao, F.; Zhao, D. *Nano Lett.* **2002**, *2*, 725.
(46) Zhang, P.; Gao, L. *J. Mater. Chem.* **2003**, *13*, 2007.
(47) Larsen, T. H.; Sigman, M.; Ghezelbash, A.; Doty, R. C.; Korgel, B. A. *J. Am. Chem. Soc.* **2003**, *125*, 5638.
(48) Mao, G.; Dong, W.; Kurth, D. G.; Mohwald, H. *Nano Lett.* **2003**, *4*, 249.
(49) Liu, Z.; Xu, D.; Liang, J.; Shen, J.; Zhang, S.; Qian, Y. *J. Phys. Chem. B* **2005**, *109*, 10699.
(50) Zhang, H. T.; Wu, G.; Chen, X.-H. *Langmuir* **2005**, *21*, 4281.
(51) Ghezelbash, A.; Korgel, B. A. *Langmuir* **2005**, *21*, 9451.
(52) Wu, C.; Yu, S.-H.; Chen, S.; Guannan Liu, G.; Liu, B. *J. Mater. Chem.* **2006**, *16*, 3326.
(53) Jiao, S.; Xu, L.; Jiang, K.; Xu, D. *Adv. Mater.* **2006**, *18*, 1174.
(54) Du, W.; Qian, X.; Ma, X.; Gong, Q.; Cao, H.; Yin, J. *Chem.—Eur. J.* **2007**, *13*, 3241.
(55) Lee, H.; Yoon, S. W.; Kim, E. J.; Park, J. *Nano Lett.* **2007**, *7*, 778.
(56) Yu, X.; Cao, C.; Zhu, H.; Li, Q.; Liu, C.; Gong, Q. *Adv. Funct. Mater.* **2007**, *17*, 1397.
(57) Lou, W.; Chen, M.; Wang, X.; Liu, W. *J. Phys. Chem. C* **2007**, *111*, 9658.
(58) Li, B.; Xie, Y.; Xue, Y. *J. Phys. Chem. C* **2007**, *111*, 12181.
(59) Wang, K.-J.; Li, G.-H.; Li, J.-X.; Wang, Q.; Chen, J.-S. *Cryst. Growth Des.* **2007**, *7*, 2265.
(60) Kuzuya, T.; Itoh, K.; Sumiyama, K. *J. Colloid Interface Sci.* **2008**, *319*, 565.
(61) Roy, P.; Mondal, K.; Srivastava, S. K. *Cryst. Growth Des.* **2008**, *8*, 1530.
(62) Du, X.-S.; Mo, M.; Zheng, R.; Lim, S.-H.; Meng, Y.; Mai, Y.-W. *Cryst. Growth Des.* **2008**, *8*, 2032.
(63) Thang, S. H.; Chong, Y. K.; Mayadunne, R. T. A.; Moad, G.; Rizzardo, E. *Tetrahedron Lett.* **1999**, *40*, 2435.
(64) Shan, J.; Pulkkinen, P.; Vainio, U.; Maijala, J.; Merta, J.; Jiang, H.; Serimaa, R.; Kauppinend, E.; Tenhu, H. *J. Mater. Chem.* **2008**, *18*, 3200.

(65) Tan, C.; Lu, R.; Xue, P.; Bao, C.; Zhao, Y. *Mater. Chem. Phys.* **2008**, *112*, 500.
(66) Yang, M.; Yang, X.; Lufeng, H.; Liu, W. *Appl. Surf. Sci.* **2008**, *255*, 1750.
(67) Wu, Y.; Wadia, C.; Ma, W.; Sadtler, B.; Alivisatos, A. P. *Nano Lett.* **2008**, *8*, 2551.
(68) Zhao, Y.; Pan, H.; Lou, Y.; Qiu, X.; Zhu, J.; Burda, C. *J. Am. Chem. Soc.* **2009**, *131*, 4253.
(69) Chen, Y. B.; Chen, L.; Wu, L. M. *Chem.—Eur. J.* **2008**, *14*, 11069.
(70) Zhu, H.; Wang, J.; Wu, D. *Inorg. Chem.* **2009**, *48*, 7099.
(71) Yang, Z.-H.; Zhang, D. P.; Zhang, W.-X.; Chen, M. *J. Phys. Chem. Solids* **2009**, *70*, 840.
(72) Han, Q.; Zhu, J.; Zhu, W.; Yang, X.; Lu, L.; Wang, X. *Mater. Lett.* **2009**, *63*, 2358.
(73) Mott, D.; Yin, J.; Engelhard, M.; Loukrakpam, R.; Chang, P.; Miller, G.; Bae, I.-T.; Chandra Das, N.; Wang, C.; Luo, J.; Zhong, C.-J. *Chem. Mater.* **2010**, *22*, 261.
(74) Basu, M.; Sinha, A. K.; Pradhan, M.; Sarkar, S.; Negishi, Y.; Pal, G.; Pal, T. *Environ. Sci. Technol.* **2010**, *44*, 6313.
(75) Jiang, D.; Hu, W.; Wang, H.; Shen, B.; Deng, Y. *J. Colloid Interface Sci.* **2011**, *357*, 317.
(76) Zou, J.; Jiang, J.; Huang, L.; Jiang, H.; Huang, K. *Solid State Sci.* **2011**, *13*, 1261.
(77) Lotfipour, M.; Machani, T.; Rossi, D. P.; Plass, K. E. *Chem. Mater.* **2011**, *23*, 3032.
(78) Chang, J.-Y.; Cheng, C.-Y. *Chem. Commun.* **2011**, *47*, 9089.
(79) Kumar, P.; Nagarajan, R. *Inorg. Chem.* **2011**, *50*, 9204.
(80) Rivest, J. B.; Fong, L.-K.; Jain, P. K.; Toney, M. F.; Alivisatos, A. P. *J. Phys. Chem. Lett.* **2011**, *2*, 2402.
(81) Machani, T.; Rossi, D. P.; Golden, B. J.; Jones, E. C.; Lotfipour, M.; Plass, K. E. *Chem. Mater.* **2011**, *23*, 5491.
(82) Sun, S.; Deng, D.; Kong, C.; Song, X.; Yang, Z. *Dalton Trans.* **2012**, *41*, 3214.
(83) Nelwamondo, S. M. M.; Moloto, M. J.; Krause, R. W. M.; Moloto, N. *Mater. Lett.* **2012**, *75*, 161.
(84) Xiong, S.; Zeng, H. C. *Angew. Chem., Int. Ed.* **2012**, *51*, 949.
(85) Abdelhady, A. L.; Ramasamy, K.; Malik, M. A.; O'Brien, P.; Haigh, S. H.; Raftery, J. *J. Mater. Chem.* **2011**, *21*, 17888.
(86) Ruth, A. A.; Young, J. A. *Colloids Surf., A* **2006**, *279*, 121.
(87) Tan, G. L.; Yang, Q.; Hommerich, U.; Seo, J. T.; Temple, D. *Opt. Mater.* **2004**, *27*, 579.
(88) Murray, C. B.; Norris, D. J.; Bawendi, M. G. *J. Am. Chem. Soc.* **1993**, *15*, 8706.
(89) Talapin, D. V.; Haubold, S.; Rogach, A. L.; Kornowski, A.; Haase, M.; Waller, H. *J. Phys. Chem. B* **2001**, *105*, 2260.
(90) Peng, Z. A.; Peng, X. G. *J. Am. Chem. Soc.* **2001**, *123*, 183.
(91) Kumar, S.; Nann, T. *Chem. Commun.* **2003**, 2478.
(92) Bunge, S. D.; Krueger, K. M.; Boyle, T. J.; Rodriguez, M. A.; Headley, T. J.; Colvin, V. L. *J. Mater. Chem.* **2003**, *13*, 1705.
(93) Mntungwa, N.; Pullabhotla, V. S. R.; Revaprasadu, N. *Mater. Chem. Phys.* **2011**, *126*, 500.
(94) Ziqubu, N.; Ramasamy, K.; Pullabhotla, V. S. R.; Revaprasadu, N.; O'Brien, P. *Chem. Mater.* **2010**, *22*, 3817.
(95) Shieh, F.; Saunders, A. E.; Korgel, B. A. *J. Phys. Chem. B* **2005**, *109* (18), 8538.
(96) Taniguchi, S.; Green, M. *J. Mater. Chem.* **2011**, *21*, 11592.
(97) Chin, P. T. K.; Stouwdam, J. W.; van Bavel, S. S.; Janssen, R. A. J. *Nanotechnology* **2008**, *19*, 205602.
(98) Dagtape, P.; Chikan, V.; Jasinki, J.; Leppert, V. L. *J. Phys. Chem. C* **2007**, *111*, 14977.
(99) Khan, M. T.; Kaur, A.; Dhawan, S. K.; Chand, S. *J. Appl. Phys.* **2011**, *110*, 044509.
(100) Ma, H.; Bai, X.; Zheng, L. *Mater. Lett.* **2012**, *66*, 212.
(101) Gong, H.; Hao, X.; Wua, Y.; Cao, B.; Xu, H.; Xu, X. *J. Solid State Chem.* **2011**, *184*, 3269.
(102) Jin, X.; Kruszynska, M.; Parisi, J.; Konly-Olesiak, J. *Nano Res.* **2011**, *4* (9), 824.
(103) Li, Y.; Jing, L.; Qiao, R.; Cao, M. *Chem. Commun.* **2011**, *47*, 9293.
(104) Rogach, A. L.; Franzl, T.; Klar, T. A.; Feldman, J.; Gaponik, N.; Lesnyak, V.; Shavel, A.; Eychmuller, A.; Rakovich, Y. P.; Donegan, J. F. *J. Phys. Chem. C* **2007**, *111*, 14628.
(105) Gaponik, N.; Talapin, D. V.; Rogach, A. L.; Hoppe, K.; Shevchenko, E. V.; Kornowski, A.; Eychmuller, A.; Waller, H. *J. Phys. Chem. B* **2002**, *106*, 7177.
(106) Wang, T.; Jin, Z.; Shi, Y.; Li, W.; Yang, J. *Cryst. Growth Des.* **2009**, *9*, 5077.
(107) Tang, Z.; Kotov, N. A.; Giersig, M. *Science* **2002**, *297*, 237.
(108) Rogach, A. L.; Katsikas, L.; Kornowski, A.; Su, D.; Eychmuller, A.; Weller, H. *Ber. Bunsen-Ges. Phys. Chem.* **1996**, *100*, 1772.
(109) Li, L.; Qian, H.; Ren, J. *Chem. Commun.* **2005**, 528.
(110) Bao, H.; Wang, E.; Dong, S. *Small* **2006**, *2*, 476.
(111) Gao, M. Y.; Kirstein, S.; Mohwald, H.; Rogach, A. L.; Kornowski, A.; Eychmuller, A.; Waller, H. *J. Phys. Chem. B* **1998**, *102*, 8360.
(112) Green, M.; Harwood, H.; Barrowman, C.; Rahman, P.; Eggeman, A.; Festry, F.; Dibson, P.; Ng, T. *J. Mater. Chem.* **2007**, *17*, 1989.
(113) Gur, I.; Fromer, N. A.; Geier, M. L.; Alivisatos, A. P. *Science* **2005**, *210*, 462.
(114) Olson, J. D.; Rodriguez, Y. W.; Yang, L. D.; Alers, G. B.; Carter, S. A. *Appl. Phys. Lett.* **2010**, *96*, 3.
(115) Mac Donald, B. I.; Martucci, A.; Rubanov, S.; Watkins, S. E.; Mulvaney, P.; Jasieniak, J. *ACS Nano* **2012**, *6*, 5995.
(116) Jasieniak, J.; Mac Donald, B. I.; Watkins, S. E.; Mulvaney, P. *Nano. Lett.* **2011**, *11*, 2856.
(117) Jiang, T.; Ozin, G. A. *J. Mater. Chem.* **1998**, *8*, 1099.
(118) Singh, J. P.; Bedi, R. K. *Thin Solid Films* **1991**, *199*, 9.
(119) Parenteau, M.; Carlone, C. *Phys. Rev. B* **1990**, *41*, 5227.
(120) Johnson, J. B.; Jones, H.; Lathan, B. S.; Parker, J. D.; Engelken, R. D.; Barber, C. *Semicond. Sci. Technol.* **1999**, *14*, 501.
(121) Radot, M. *Rev. Phys. Appl.* **1977**, *18*, 345.
(122) Pramanik, P.; Basu, P. K.; Biswas, S. *Thin Solid Films* **1987**, *150*, 269.
(123) Brownson, J. R. S.; Georges, C.; Larramona, G.; Jacob, A.; Delatouche, B.; Levy-Clement, C. *J. Electrochem. Soc.* **2008**, *155*, D40.
(124) Cheng, S.; Chen, G.; Chen, Y.; Huang, C. *Opt. Mater.* **2006**, *29*, 439.
(125) Alpen, U. V.; Fenner, J.; Gmelin, E. *Mater. Res. Bull.* **1975**, *10*, 175.
(126) Ristov, M.; Sinadinovski, G.; Grozdanov, I.; Mitreski, M. *Thin Solid Films* **1989**, *173*, 53.
(127) Hickey, S. G.; Waurisch, C.; Rellinghaus, B.; Eychmuller, A. *J. Am. Chem. Soc.* **2008**, *130*, 14978.
(128) Liu, H. T.; Liu, Y.; Wang, Z.; He, P. *Nanotechnology* **2010**, *21*, 105707.
(129) Ning, J. J.; Men, K. K.; Xiao, G. J.; Wang, L.; Dai, Q. Q.; Zou, B.; Liu, B. B.; Zou, G. T. *Nanoscale* **2010**, *2*, 1699.
(130) Xu, Y.; Al-Salim, N.; Bumby, C. W.; Tilley, R. D. *J. Am. Chem. Soc.* **2009**, *131*, 15990.
(131) Zhang, Y.; Lu, J.; Shen, S.; Xu, H.; Wang, Q. *Chem. Commun.* **2011**, *47*, 5226.
(132) Han, Q.; Wang, M.; Zhu, J.; Wu, X.; Lu, L.; Wang, X. *J. Alloys Compd.* **2011**, *509*, 2180.
(133) Deng, Z.; Han, D.; Liu, Y. *Nanoscale* **2011**, *3*, 4346.
(134) Ren, L.; Jin, Z.; Wang, W.; Liu, H.; Lai, J.; Yang, J.; Hong, Z. *Appl. Surf. Sci.* **2011**, *258*, 1353.
(135) Greyson, E. C.; Barton, J. E.; Odom, T. W. *Small* **2006**, *2*, 368.
(136) Chakrabarti, A.; Lu, J.; McNamara, A. M.; Kuta, L. M.; Stanley, S. M.; Xiao, Z.; Maguire, J. A.; Hosmane, N. S. *Inorg. Chim. Acta* **2011**, *374*, 627.
(137) Sohila, S.; Rajalakshmi, M.; Ghosh, C.; Arora, A. K.; Muthamizhchelvan, C. *J. Alloys Compd.* **2011**, *509*, 5843.
(138) Jun, Y.-W.; Choi, J.-S.; Cheon, J. *Angew. Chem., Int. Ed.* **2006**, *45*, 3414.

(139) Joo, J.; Na, H. B.; Yu, T. Y.; Yu, J. H.; Kim, Y. W.; Wu, F.; Zhang, J. Z.; Hyeon, T. *J. Am. Chem. Soc.* **2003**, *125*, 11100.
(140) Cademartiri, L.; Bertolotti, J.; Sapienza, R.; Wiersma, D. S.; Freymann, G. V.; Ozin, G. A. *J. Phys. Chem. B* **2006**, *110*, 671.
(141) Liu, J.; Yu, H.; Wu, Z.; Wang, W.; Peng, J.; Cao, Y. *Nanotechnology* **2008**, *19*, 345602.
(142) Hines, M. A.; Scholes, G. D. *Adv. Mater.* **2003**, *15* (21), 1844.
(143) Trindade, T.; O'Brien, P.; Zhang, X.; Motevalli, M. *J. Mater. Chem.* **1997**, *7*, 1011.
(144) Lee, S. M.; Jun, Y. W.; Cho, S. N.; Cheon, J. W. *J. Am Chem. Soc.* **2002**, *124*, 11244.
(145) Akhtar, J.; Malik, M. A.; O'Brien, P.; Helliwell, M. *J. Mater. Chem.* **2010**, *20*, 6116.
(146) Aktar, J.; Malik, M. A.; O'Brien, P.; Wijayantha, K. G. U.; Dharmadasa, R.; Hardman, S. J. O.; Graham, D. M.; Spencer, B. F.; Stubbs, S. K.; Flavell, W. R.; Binks, D. J.; Sirotti, F.; El Kazzi, M.; Silly, M. *J. Mater. Chem.* **2010**, *20*, 2336.
(147) Yu, D.; Chen, Y.; Li, B.; Chen, X. *Mater. Lett.* **2009**, *63*, 2317.
(148) Qiu, W.; Xu, M.; Chen, F.; Yang, X.; Nan, Y.; Chen, H. *CrystEngComm* **2011**, *13*, 4689.
(149) Nyamen, L. D.; Rajasekhar Pullabhotla, V. S. R.; Nejo, A. A.; Ndifon, P. T.; Warner, J. H.; Revaprasadu, N. *Dalton Trans.* **2012**, *41*, 8297.
(150) Salvati-Niasari, M.; Sobhani, A.; Davar, F. *J. Alloys Compd.* **2010**, *507*, 77.
(151) Shan-Sun, S.; Han, Q.-F.; Wu, X.-D.; Zhu, J.-W.; Wang, X. *Mater. Lett.* **2011**, 3344.
(152) Mandal, T.; Piburn, G.; Stavila, V.; Rusakova, I.; Ould-Ely, T.; Colson, A. C.; Whitmire, H. K. *Chem. Mater.* **2011**, *23*, 4158.
(153) Warner, J. H.; Cao, H. *Nanotechnology* **2008**, *19*, 305605.
(154) Xu, F.; Ma, X.; Gerlein, L. P.; Cloutier, S. G. *Nanotechnology* **2011**, *22*, 265604.
(155) Neji, A. O.; Nejo, A. A.; Pullabhotla, P. V. S. R.; Revaprasadu, N. *J. Alloys Compd.* **2012**, *537*, 19.
(156) Duahem, T.; Lou, W.; Wang, X.; Xue, Q. *Colloids Surf., A* **2007**, *86*, 310.
(157) Sun, J.-Q.; Shen, X.-P.; Guo, L.-J.; Chen, K.-M.; Liu, Q. *Physica E* **2009**, *41*, 1527.
(158) Zhao, Y.; Liao, X.-H.; Hong, J.-M.; Zhu, J.-J. *Mater. Chem. Phys.* **2004**, *87*, 149.
(159) Patel, J. D.; Mighri, F.; Ajji, A.; Chaudhuri, T. K. *Mater. Chem. Phys.* **2012**, *132*, 747.
(160) Qiu, W.; Xu, M.; Chen, F.; Yang, X.; Nan, Y.; Chen, H. *CrystEngComm* **2011**, *13*, 4689.
(161) Kane, S. R.; Cohen, R. E.; Silbey, R. *Chem. Mater.* **1996**, *8*, 1919.
(162) Kane, S. R.; Cohen, R. E.; Silbey, R. J. *Phys. Chem.* **1996**, *100*, 7928.
(163) Wang, S.; Yang, S. *Langmuir* **2000**, *16*, 389.
(164) Parvathy, N. N.; Pajonk, G. M.; Rao, A. V. J. *Cryst. Growth* **1997**, *179*, 249.
(165) Martucci, A.; Innocenzi, P.; Flick, J.; Mackenzie, J. D. *Non-Cryst. Solids* **1999**, *244*, 55.
(166) Watt, A. A. R.; Meredith, P.; Riches, J. D.; Atkinson, S.; Rubinsztein-Dunlop, H. *Curr. Appl. Phys.* **2004**, *4*, 320.
(167) Watt, A. A. R.; Blake, D.; Warner, J. H.; Thomsen, E. A.; Tavenner, E. L.; Rubinsztein-Dunlop, H.; Meredith, P. *J. Phys. D* **2005**, *38*, 20.
(168) Watt, A. A. R.; Meredith, P.; Rubinsztein-Dunlop, H. *Chem. Commun.* **2004**, 2334.
(169) Stavrinadis, A.; Beal, R.; Smith, J. M.; Assender, H. E.; Watt, A. A. R. *Adv. Mater.* **2008**, *20*, 3105.
(170) Stavrinadis, A.; Xu, S.; Warner, J. H.; Hutchison, J. L.; Smith, J. M.; Watt, A. A. R. *Nanotechnology* **2009**, *20*, 445608.
(171) Yu, D.; Chen, Y.; Li, B.; Chen, X. *Mater. Lett.* **2009**, *63*, 2317.
(172) Li, C.; Zhao, Y.; Li, F.; Shi, Z.; Feng, S. *Chem. Mater.* **2010**, *22*, 1901.
(173) Xiang, J.; Cao, H.; Wu, Q.; Zhang, S.; Zhang, X. *Cryst. Growth Des* **2008**, *11*, 3935.
(174) Navaneethan, M.; Nisha, K. D.; Ponnusamy, S.; Muthamizhchelvan, C. *Mater. Chem. Phys.* **2009**, *117*, 443.
(175) Fang, Z.; Wang, Q.; Wang, X.; Zhu, B.; Fan, F.; Wang, C.; Liu, X. *Cryst. Res. Technol.* **2012**, *47* (6), 635.
(176) Bu, J.; Nie, C.; Liang, J.; Sun, L.; Xie, Z.; Wu, Q.; Lin, C. *Nanotechnology* **2011**, *22*, 125602.
(177) Salavati-Niasari, M.; Ghanbari, D. *Particuology* **2012**, *10*, 628.
(178) Salavati-Niasari, M.; Ghanbari, D.; Loghman-Estarki, M. R. *Polyhedron* **2012**, *35*, 149.
(179) Li, G.; Li, C.; Tang, H.; Cao, H.; Chen, J. *Mater. Res. Bull.* **2011**, *46*, 1072.
(180) Berhanu, D.; Govender, K.; Smythe-Boyle, D.; Archbold, M.; Halliday, D. P.; O'Brien, P. *Chem. Commun.* **2006**, 4706.
(181) Lu, Q.; Gao, F.; Komarneni, S. *J. Am. Chem. Soc.* **2004**, *126*, 54.
(182) Gao, F.; Lu, Q.; Komarneni, S. *Chem. Commun.* **2005**, 531.
(183) Liu, Z.; Xu, D.; Liang, J.; Lin, W.; Yu, W.; Qian, Y. *J. Solid State Chem.* **2005**, *178*, 950.
(184) Jiang, J.; Yu, S. H.; Yao, W. T.; Ge, H.; Zhang, G. Z. *Chem. Mater.* **2005**, *17*, 6094.
(185) Zhang, B.; Ye, X.; Hou, W.; Zhao, Y.; Xie, Y. *J. Phys. Chem. B* **2006**, *110*, 8978.
(186) Ota, J.; Srivastava, S. K. *J. Phys. Chem. C* **2007**, *111*, 12260.
(187) Cademartiri, L.; Malakooti, R.; O'Brien, P. G.; Migliori, A.; Petrov, S.; Kherani, N. P.; Ozin, G. A. *Angew. Chem., Int. Ed.* **2008**, *47*, 3814.
(188) Cademartiri, L.; Guerin, G.; Bishop, K. J. M.; Winnik, M. A.; Ozin, G. A. *J. Am. Chem. Soc.* **2012**, *134*, 9327.
(189) Thomson, J. W.; Cademartiri, L.; MacDonald, M.; Petrov, S.; Calestani, G.; Zhang, P.; Ozin, G. A. *J. Am. Chem. Soc.* **2010**, *132*, 9058.
(190) Zhou, H.; Xiong, S.; Wei, L.; Xi, B.; Zhu, Y.; Qian, Y. *Cryst. Growth Des.* **2009**, *9*, 3862.
(191) Tian, L.; Tan, H. Y.; Vittal, J. J. *Cryst. Growth Des.* **2008**, *8*, 734.
(192) Han, Q. F.; Chen, J.; Yang, X. J.; Lu, L.; Wang, X. *J. Phys. Chem. C* **2007**, *111*, 14072.
(193) Lou, W.; Chen, M.; Wang, X.; Liu, W. *Chem. Mater.* **2007**, *19*, 872.
(194) Wang, Q.; Wang, X.; Lou, W.; Hao, J. *New J. Chem.* **2010**, *34*, 1930.
(195) Shen, X. P.; Yin, G.; Zhnag, W.-L.; Xu, Z. *Solid State Commun.* **2006**, *140*, 116.
(196) Jain, A. K.; Sharma, V.; Bohra, R.; Sukumar, A. A.; Raju, V. S.; Drake, J. E.; Hursthouse, M. B.; Light, M. E. *J. Organomet. Chem.* **2006**, *691*, 4128.
(197) Xie, G.; Qiao, Z. P.; Zeng, M. H.; Chen, X. M.; Gao, S. L. *Cryst. Growth Des.* **2004**, *4*, 513.
(198) Stavila, V.; Whitmire, K. H.; Rusakova, I. *Chem. Mater.* **2009**, *21*, 5456.
(199) Shi, L.; Gu, D.; Li, W.; Han, L.; Wei, H.; Tu, B.; Che, R. *J. Alloys Compd.* **2011**, *509*, 9382.
(200) Panthani, M. G.; Akhavan, V.; Goodfellow, B.; Schmidtke, J. P.; Dunn, L.; Dodabalapur, A.; Barbara, P. F.; Korgel, B. A. *J. Am. Chem. Soc.* **2008**, *130*, 16770.
(201) Zhong, H.; Zhou, Y.; Ye, M.; He, Y.; Ye, J.; He, C.; Yang, C.; Li, Y. *Chem. Mater.* **2008**, *20*, 6434.
(202) Allen, P. M.; Bawendi, M. G. *J. Am. Chem. Soc.* **2008**, *130*, 9240.
(203) Malik, M. A.; O'Brien, P.; Revaprasadu, N. *Adv. Mater.* **1999**, *11*, 1441.
(204) Pan, D.; An, L.; Sun, Z.; Hou, W.; Yang, Y.; Yang, Z.; Lu, Y. *J. Am. Chem. Soc.* **2008**, *130*, 5621.
(205) Koo, B.; Patel, R. N.; Korgel, B. A. *Chem. Mater.* **2009**, *21*, 1962.
(206) Batabyal, S. K.; Tian, L.; Venkatram, N.; Ji, W.; Vittal, J. J. *J. Phys. Chem. C* **2009**, *113*, 15037.
(207) Kruszynska, M.; Borchert, H.; Parisi, J.; Kolny-Olesiak, J. *J. Am. Chem. Soc.* **2010**, *132*, 15976.
(208) Ford, G. M.; Guo, Q.; Agrawal, R.; Hillhouse, H. W. *Thin Solid Films* **2011**, *520*, 523.

(209) Li, L.; Pandey, A.; Werder, D. J.; Khana, B. P.; Pietryga, J. M.; Klimov, V. I. *J. Am. Chem. Soc.* **2011**, *133*, 1176.
(210) Song, W. S.; Yang, H. *Chem. Mater.* **2012**, *24*, 1961.
(211) Bao, N.; Qiu, X.; Wang, Y.-H. A.; Zhou, Z.; Lu, X.; Grimes, C. A.; Gupta, A. *Chem. Commun.* **2011**, *47*, 9441.
(212) Shen, F.; Que, W.; Zhong, P.; Zhang, J.; Yin, X. *Colloids, Surf. A* **2011**, *392*, 1.
(213) He, J.-J.; Zhou, W.-H.; Guo, J.; Li, M.; Wu, S.-X. *CrystEngComm* **2012**, *14*, 3638.
(214) Malik, S. N.; Mahboob, S.; Haider, N.; Malik, M. A.; O'Brien, P. *Nanoscale* **2011**, *3*, 5132.
(215) Abdelhady, A. L.; Malik, M. A.; O'Brien, P. *J. Mater. Chem.* **2012**, *22*, 3781.
(216) Huang, W.-C.; Tseng, C.-H.; Chang, S.-H.; Tuan, H.-Y.; Chiang, C.-C.; Lyu, L.-M.; Huang, M. H. *Langmuir* **2012**, *28*, 8496.
(217) Guo, Q.; Ford, G. M.; Hillhouse, H. W.; Agrawal, R. *Nano Lett.* **2009**, *9*, 3060.
(218) Lee, J. H.; Chang, J.; Cha, J.-H.; Lee, Y.; Han, J. E.; Jung, D.-Y.; Choi, E. C.; Hong, B. *Eur. J. Inorg. Chem.* **2011**, 647.
(219) Ahn, S.; Kim, K.; Yoon, K. *Curr. Appl Phys.* **2008**, *8*, 766.
(220) Wang, Y.-H. A.; Zhang, X.; Bao, N.; Lin, B.; Gupta, A. *J. Am. Chem. Soc.* **2011**, *133*, 11072.
(221) Jiang, C.; Lee, J.-S.; Talapin, D. V. *J. Am. Chem. Soc.* **2012**, *134*, 5010.
(222) Chang, S.-H.; Chiang, M.-Y.; Chiang, C.-C.; Yuan, F.-W.; Chen, C.-Y.; Chiu, B.-C.; Kao, T.-L.; Lai, C.-H.; Tuan, H.-Y. *Energy Environ. Sci.* **2011**, *4*, 4929.
(223) Wooten, A. J.; Werder, D. J.; Williams, D. J.; Casson, J. L.; Hollingsworth, J. A. *J. Am. Chem. Soc.* **2009**, *131*, 16177.
(224) Barkhouse, D. A. R.; Gunawan, O.; Gokmen, T.; Todorov, T. K.; Mitzi, D. B. *Prog. Photovoltaics* **2012**, *20*, 6.
(225) Ramasamy, K.; Malik, M. A.; O'Brien, P. *Chem. Commun.* **2012**, *48*, 5703.
(226) Singh, A.; Geaney, H.; Laffir, F.; Ryan, K. M. *J. Am. Chem. Soc.* **2012**, *134*, 2910.
(227) Regulacio, M. D.; Ye, C.; Lim, S. H.; Bosman, M.; Ye, E.; Chen, S.; Xu, Q.-H.; Han, M.-Y. *Chem.—Eur. J.* **2012**, *18*, 3127.
(228) Shavel, A.; Cadavid, D.; Ibanez, M.; Carrete, A.; Cabot, A. *J. Am. Chem. Soc.* **2012**, *134*, 1438.
(229) Khare, A.; Wills, A. W.; Ammerman, L. M.; Norris, D. J.; Aydil, E. S. *Chem. Commun.* **2011**, *47*, 11721.
(230) Riha, S. C.; Parkinson, B. A.; Prieto, A. L. *J. Am. Chem. Soc.* **2011**, *133*, 15272.
(231) Ou, K.-L.; Fan, J.-C.; Chen, J.-K.; Huang, C.-C.; Chen, L.-Y.; Ho, J.-H.; Chang, J.-Y. *J. Mater. Chem.* **2012**, *22*, 14667.
(232) Su, Z.; Yan, C.; Tang, D.; Sun, K.; Han, Z.; Liu, F.; Lai, Y.; Li, J.; Liu, Y. *CrystEngComm* **2012**, *14*, 782.
(233) Tian, Q.; Xu, X.; Han, L.; Tang, M.; Zou, R.; Chen, Z.; Yu, M.; Yang, J.; Hu, J. *CrystEngComm* **2012**, *14*, 3847.
(234) Saha, S. K.; Guchhait, A.; Pal, A. J. *Phys. Chem. Chem. Phys.* **2012**, *14*, 8090.
(235) Jiang, H.; Dai, P.; Feng, Z.; Fan, W.; Zhan, J. *J. Mater. Chem.* **2012**, *22*, 7502.
(236) Shavel, A.; Arbiol, J.; Cabot, A. *J. Am. Chem. Soc.* **2010**, *132*, 4514.
(237) Wang, J.-J.; Hu, J.-S.; Guo, Y.-G.; Wan, L.-J. *NPG Asia Mater.* **2012**, DOI: DOI: 10.1038/am/2012.2.
(238) Liu, Y.; Yao, D.; Shen, L.; Zhang, H.; Zhang, X.; Yang, B. *J. Am. Chem. Soc.* **2012**, *134*, 7207.